Results: Precision-Recall (PR) curves were used to evaluate the WDM-CBIR and compared against a CBIR system that used the Euclidian distance metric (EDM-CBIR) with the same texture features. Figure 1a clearly shows that our WDM-CBIR outperformed the EDM-CBIR on a cohort of 58 prostate cancer studies. The average area under the curve for the WDM-CBIR was 0.95 compared to 0.72 for the EDM-CBIR.

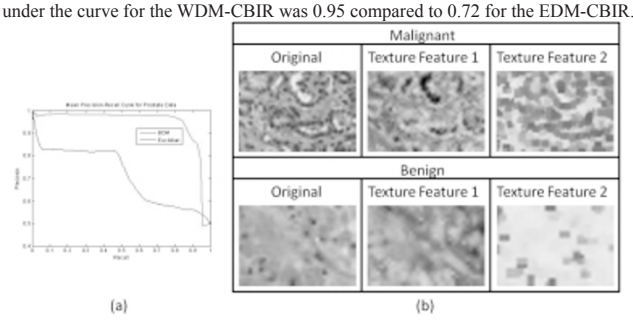

Figure 1: (a) PR Curves for WDM and EDM CBIR systems evaluated on prostate biopsy studies. (b) Representative examples of malignant and benign regions with corresponding texture representations.

Conclusions: We introduced a new WDM-CBIR system that differentially weights individual image attributes based on their discriminatory performance. WDM-CBIR outperformed the EDM-CBIR on 58 prostate cancer studies. WDM-CBIR can be extended and applied to other domains within digital pathology.

1454 Telecytopathology for Rapid Preliminary Diagnosis of Ultrasound-Guided Fine Needle Aspiration of Thyroid Nodules.

IN Swati, R Izquierdo, R Kasturi, KK Khurana. SUNY Upstate Medical University, Syracuse, NY.

Background: Onsite evaluation of ultrasound-guided fine needle aspiration (USGFNA) is essential to procure adequate samples and provide initial assessment. We present our experience with onsite evaluation of USGFNA using telecytopathology.

Design: Real time images of Diff Quik stained cytology smears were obtained with an Olympus Digital camera attached to an Olympus CX41 microscope and transmitted via ethernet by cytotechnologist to a pathologist who rendered preliminary diagnosis while communicating with onsite cytotechnologist over the phone. Accuracy of preliminary diagnosis was compared with final diagnosis, retrospectively. Kappa statistic was used to compare agreements between telecytopathology preliminary diagnoses versus final diagnoses.

Results: A total of 51 patients (mean age 48.9 yr) underwent USG-FNA of 65 thyroid nodules. Preliminary diagnoses of benign, suspicious/ malignant and unsatisfactory were 77%, 5% and 18% respectively. Of the 50 cases initially reported as benign all remained benign on the final cytology. All suspicious / malignant cases on initial cytology corresponded with a malignant diagnosis on final cytology. Of the 12 cases that were initially interpreted as unsatisfactory only 2 were reclassified as benign on final diagnosis. There was excellent agreement between telecytopathology and final cytologic evaluation (Kappa value 85%). Presence of additional material on pap stained slides was the main reason for discrepancy accounting for two discrepant cases in the unsatisfactory category.

Conclusions: This retrospective study demonstrates onsite telecytopathology evaluation of thyroid USG-FNA is highly accurate compared with final cytologic evaluation. It allows pathologists to use their time more efficiently and makes onsite evaluation at a remote site possible.

Kidney

1455 The Renal Distribution of Iron (Fe) in Primary Hemochromatosis: An Autopsy Study.

V Ananthanarayanan, S Meehan, A Chang. University of Chicago, IL.

Background: The distribution of iron (Fe) within the renal parenchyma of patients with primary hemochromatosis has not been studied. We conducted this study to determine the spectrum of Fe distribution in autopsy kidneys in the setting of primary hemochromatosis. We also evaluated whether the presence of the H63D or C282Y mutations, the most common mutations in hereditary hemochromatosis, resulted in a difference in iron distribution in the kidneys of affected patients.

Design: We identified 12 cases of hemochromatosis in our pathology database from 1993-2010, after excluding cases of hemosiderosis and secondary hemochromatosis. H&E and Prussian blue stain were analyzed and the distribution of Fe in the various compartments of the renal parenchyma was assessed. These findings were correlated with the available clinical and mutation data (H63D and C282Y).

Results: Of the 12 cases of primary hemochromatosis, there were 8 males and 4 females with an average age of 54 years (range: 32 to 73 years). Eight patients had histologically proven cirrhosis while 4 patients had increased Fe deposition in the hepatocytes. In the kidneys, there typically was more staining for Fe in the cortex than the medulla. Within the cortex, Fe was noted in the glomeruli, proximal convoluted tubules (PCT) and distal nephron segments. In most cases, the staining in the distal nephron segments, when present, was more intense than the PCT. Podocytes and parietal epithelial cells were the primary cells in glomeruli with Fe, but no mesangial or glomerular endothelial staining was identified. One case showed the presence of Fe in only glomeruli limited to the podocytes. Few cases had additional rare interstitial and endothelial staining. Furthermore, patchy staining of the glomerular basement membranes in globally sclerotic glomeruli, Bowman's capsules and tubular basement membranes was also noted in a subset of cases. In the four cases where mutation data was available, no difference in Fe distribution was observed.

Conclusions: This is the first study to describe the distribution of Fe in autopsy kidneys of primary hemochromatosis patients. Most cases showed a predominant staining pattern in the cortex with a greater distribution in the distal nephron segments. Regardless, of the involved compartment, Fe deposition was patchy and irregular. The persistence of iron deposition in the podocytes could be due to their terminal differentiation, but this would require further study.

1456 Identification of a Potential Marker of Glomerular Fibrogenesis in Childhood Nephrotic Syndrome.

MM Cajaiba, R Ayoob, R Houston, SI Bastacky, P Baker. Nationwide Children's Hospital, Columbus, OH; University of Pittsburgh, PA.

Background: Minimal change disease (MCD) and focal segmental glomerulosclerosis (FSGS) are the major causes of pediatric nephrotic syndrome (NS). Most MCD cases respond to steroids, whereas FSGS tends to be resistant and progress to global sclerosis leading to chronic renal disease. The reversible nature of MCD is thought to reflect transient podocyte damage due to increased circulating cytokines, whereas FSGS would correspond to irreversible podocyte damage with activation of TGF-β-mediated apoptosis and fibrogenesis. Markers of fibrogenesis that could help to define the pathogenesis and prognosis in these cases have not been clearly identified. One of the downstream targets of TGF-β signalling is Sox9, a transcription factor involved in normal skeletal development and pathological fibrogenesis. Recent experimental studies showed increased levels of both Sox9 and TGF-β mRNA in FSGS, and increased glomerular collagen IV accumulation triggered by TGF-β-induced Sox9 expression. The aim of this study is to investigate Sox9 as a potential indicator of glomerular fibrogenesis in NS.

Design: 29 renal needle biopsies performed in children with NS were selected; 15 were diagnosed as FSGS and 14 as MCD. 10 renal biopsies from healthy living transplant donors were used as normal controls. Immunohistochemical stains with an antibody against Sox-9 were performed on representative slides from each case. Specimens with sampling of 5 or more glomeruli were considered adequate. Sox9 nuclear staining was recorded as positive/negative in glomeruli (mesangial cells/podocytes), and as percentage of stained cells in parietal and tubular epithelial cells (PEC/TEC).

Results: Ages ranged from 1-18 years, with 14 males and 15 females. 5 cases (3 FSGS and 2 MCD) were excluded due to sampling inadequacy. None (0/10) of the normal controls showed glomerular staining. 7/12 (58.3%) FSGS cases had positive glomerular staining (seen in segmentally sclerotic and non-sclerotic glomeruli) versus 1/12 (8.3%) MCD cases (p=0.0136). Sox9 stained 0-10% of TEC and PEC in all controls (100%) and most MCD (67%), and 10-50% in most FSGS cases (67%).

Conclusions: Glomerular Sox9 expression was significantly more frequent in FSGS than MCD, suggesting a potential use for this protein as a diagnostic/prognostic marker of fibrogenesis in NS. A larger patient sample is needed to confirm these observations, to establish a possible relationship between Sox9 staining and poor outcome in MCD, and an association between tubular Sox9 staining and chronic parenchymal changes.

1457 Clinical Implications of Polyomavirus-Associated Nephropathy after Renal Transplantation.

HP Cathro, JC Gardenier, CD Sifri, DS Keith, RG Sawyer, KL Brayman, H Bonatti. University of Virginia, Charlottesville; Vanderbilt University, Nashville, TN.

Background: BK virus nephropathy (BKVN) develops in ~5% of renal transplants (RT), causing graft loss in 15-80% of cases within 5 years. Most studies suggest that the majority of BKVN occurs during the first post-transplant (PT) year. We noticed an increasing number of cases of late-onset BKVN and conducted a retrospective study.

Design: All renal specimens from patients with biopsy-proven BKVN from 2000-2009 at a single institution were reviewed.

Results: Of 846 RT recipients, 18 had biopsy-proven BKVN (2.1%), 4 of whom had also received pancreatic transplants. The median age of 12 males and 6 females was 52.2 yr (range 27.9-63.8 yr), and the median time PT was 20.1 mn (range 3.2-80.4 mn), with only 4 or 22%, <1 yr out. Fourteen patients were on standard immunosuppression (IS). Screening for BK virus was erratically administered due to geographical/logistical constraints. Five patients had prior biopsy proven episodes of acute rejection and 13 patients (72%) had received intensive prior IS, usually for acute rejection (n=10) or for subsequent pancreas transplantation. Fourteen patients were treated with antiviral therapy, +/- IVIG, +/- IS taper, and single patients were treated with IVIG or IS taper alone. One patient died after returning to dialysis, and 17 were alive at an average of 3.4 yr follow up. Seven of these had returned to dialysis (41%), and 5 had a serum creatinine >2 mg/dL (29%). Only 5 patients had good graft function (29%).

Conclusions: Retrospective analysis of BKVN at a single institution during the current IS era demonstrated 78% of cases occurring after the first PT year, and 39% after the second PT year. Inconsistent screening and over-IS may be playing a role. The poor outcome of 72% of the BKVN cases is in part due to late diagnosis at a severe stage of disease. Late onset BKVN is an underrecognized cause of graft loss and dysfunction, and rigorous screening followed by tapering of IS on positive testing, should be emphasized beyond the first year post-transplantation.

1458 Membranoproliferative Glomerulonephritis and Less Characterized Etiological Factors.

S Cheemalavaagu, SH Woo, A Mahapatra, N Kambham. Stanford University, CA; Kaiser Permanente, Santa Clara.

Background: Membranoproliferative glomerulonephritis (MPGN types I, III) is an uncommon cause of nephrotic syndrome (NS) in adults, is often associated with immune complex deposits and characterized by mesangial proliferation and reduplication of glomerular basement membranes. Majority of MPGN cases are secondary to autoimmune diseases, cryoglobulins, Hepatitis C infection, and dysproteinemias. Other causes of MPGN are less well studied and many are categorized as idiopathic.

Design: Pathology database was searched (2000-09) for renal biopsies with a diagnosis of MPGN in adults. Patients with clinical or serological evidence of systemic lupus erythematosus (ANA), cryoglobulinemia, Heptitis C/B infection, dysproteinemia (SPEP, UPEP) or lymphoproliferative disorders were excluded. Clinical data including presentation, laboratory investigations and follow up were obtained and all biopsies were reviewed for histological parameters. In addition to routine immunofluorescence staining (including K, L light chains), IgG subtyping was studied (IgG1-4).

Results: A total of 30 patients met our inclusion criteria and the mean age at presentation was 57 years (range 20-85). Two thirds of the patients presented with full NS while most others had non-nephrotic proteinuria. Renal insufficiency was common and one patient presented with acute renal failure. The amount of 24 hour proteinuria had a significant correlation with poor renal function (serum creatinine) (R=0.65, P= 0.001) while crescents, % glomerulosclerosis and interstitial fibrosis did not correlate with renal function. Except in one, immune deposits were evident in all patients either by immunofluorescence or ultrastructural examination. C3 deposits were common followed by IgG and IgM. K/L light chain restriction was detected in 12 patients (9K; 3L) and IgG subclass was monoclonal in nine patients (IgG3: 8; IgG2:1) and oligoglonal in 4 others. The possible etiological factors based on clinical history and follow up include cirrhosis, portocaval shunts, autoimmune hemolytic anemia, drugs and familial forms.

Conclusions: MPGN secondary to less characterized etiologies includes a broad spectrum and the cause may often be elusive. The light chain and IgG subtype restriction may be observed despite lack of monoclonal gammopathy and may result from chronic antigenic/immune stimulation. Histologic parameters were not strongly correlated with renal function.

1459 HLA-DR Immunohistochemistry Quantitation in Renal Allograft Biopsies: Objective Discrimination of Rejection and Other Pathologic Processes.

AB Farris, J Kong, C Chisolm, HM Gebel, RA Bray, C Cohen, DJ Brat, JH Saltz, AD Kirk, R Hennigar. Emory University, Atlanta, GA; Emory University, Atlanta.

Background: Histologic renal allograft biopsy (bx) assessment methods (e.g., the Banff criteria), although historically useful, largely rely on semi-quantitative, granular criteria, sometimes making the appreciation of subtle pathologic differences difficult. Human leukocyte antigen (HLA)-DR expression has been shown in renal allografts, particularly bxs with rejection. We investigated the utility of renal allograft bx assessment using HLA-DR immunohistochemistry (IHC) whole slide image (WSI) analysis.

Design: IHC was performed with a commercially-available HLA-DR antibody on bxs containing allograft rejection, polyomavirus nephritis (PVN), a borderline pattern, normal donor tissue, and stable allografts. HLA-DR WSIs obtained using an Olympus Nanozoomer scanner were quantitated with regard to total and cortical renal parenchymal staining using the Aperio Imagescope Positive Pixel Count algorithm, yielding a % of parenchyma with HLA-DR positivity.

Results: Highest HLA-DR positivity was seen in allograft rejection bxs [Table]. Elevated levels were also seen in PVN, followed by borderline cases. A baseline HLA-DR level was present in normal donor bxs, and the lowest levels were in stable allografts. Differences were not significant between rejection and polyomavirus nephritis; however HLA-DR levels in rejection and PVN were significantly higher than stable and normal donor bxs. Rejection but not PVN was significantly higher than borderline. Linear regression showed a direct correlation between total and cortical HLA-DR ($R^2 = 0.98$, $P < 0.0001$).

Type	HLA-DR total parenchymal positivity (%) [Mean ± S.D.]	Comparison (T-test)
Rejection (n = 15)	62.2 ± 16.2	***, *, •
Antibody-mediated rejection (n=3)	68.6 ± 9.3	***, *, •
Cellular rejection (n =12)	60.6 ± 17.4	***, *, •
PVN (n = 3)	60.6 ± 8.1	**, ^
Borderline (n = 2)	36.1 ± 10.4	
Normal donor (n = 4)	33.6 ± 18.5	
Stable allograft (n =3)	15.0 ± 4.4	

S.D.: standard deviation, ***: P < 0.0005 vs. stable, **: P = 0.001 vs. stable, *: P < 0.01 vs. normal donor, ^: P = 0.03 vs. normal donor, •: P < 0.05 vs. borderline

Conclusions: Our data suggest that HLA-DR IHC quantitation has a potential for utility in objectively measuring the immunologic activation of allografts, particularly when combined with emerging WSI segmentation algorithms. Future studies using additional histologic, IHC, and molecular markers may prove useful.

1460 Parietal Epithelial Cell Activation Distinguishes Early Recurrence of FSGS in the Transplant from Minimal Change Disease.

H Fatima, MJ Moeller, B Smeets, H-C Yang, AB Fogo. Vanderbilt University Medical Center, Nashville, TN; University Hospital of RWTH Aachen University, Germany.

Background: Podocyte (PODO) loss is a key factor leading to glomerulosclerosis. Podocytes have limited regenerative capacity. Parietal epithelial cells (PEC) have been proposed as niche stem cells that can transition to podocytes. CD44 is a glycoprotein involved in cell adhesion and migration and is a marker for activated PEC. We investigated whether activated PEC contribute to pathogenesis of recurrent FSGS in transplant.

Design: A total of 25 transplant renal biopsies from 12 patients with recurrent FSGS and four cases of minimal change disease (MCD) were stained for CD44. Of the 25 biopsies of recurrent FSGS, 16 early biopsies had only extensive foot process effacement (FPE) by electron microscopy and no segmental sclerosis and 9 later biopsies had segmental sclerosis. There were a total of 94, 111 and 53 glomeruli in MCD, FPE only and segmental sclerosis cases, respectively. 10 of 53 glomeruli in segmental sclerosis cases had segmental lesions. In each biopsy individual glomeruli were evaluated for the number of epithelial cells staining for CD44 along Bowman's capsule, in anatomical PEC location, and over the glomerular tuft, in anatomical PODO location.

Results: In MCD cases on average 0.05% of glomeruli stained positive for CD44 in PODO location, and 0.01% of glomeruli showed positive staining in PEC location. FPE only cases showed significantly increased positivity in PODO location, on average 0.34 vs 0.06 of glomeruli positive in MCD ($p < 0.01$) and trend for increased CD44 positivity in PEC location, 0.06 vs 0.01 in MCD ($p=0.072$). In segmental sclerosis cases, there were on average 0.8 positive cells in PODO location in glomeruli without segmental lesion, compared to 4.9 positive cells/ glomerulus in glomeruli with segmental lesions, with most positive cells located in the lesional area. In contrast, average CD44 positive cells in PEC location were similar in glomeruli with (2.8) or without lesions (1.6).

Conclusions: We conclude that there is significantly increased PEC activity in evolving FSGS vs MCD and this may distinguish MCD from early FSGS. Whether the PEC activation is causal and contributes to sclerosis in the pathogenesis of idiopathic FSGS or is a regenerative/ repair response to replace injured podocytes or both, awaits further study.

1461 Acute Glomerulitis with Neutrophils May Underscore the Development of Glomerular Basement Membrane Multi-Lamination in Transplant Glomerulopathy.

JP Gaut, J Shen, M DeGuire, C Klein, H Liapis. Washington University School of Medicine, St. Louis, MO.

Background: Acute glomerulitis (GL) in allograft biopsies is a distinct form of acute glomerular rejection, often seen in the early post-transplant period in association with antibody mediated rejection. A correlation with worse graft survival was previously reported. GL may also accompany transplant glomerulopathy (TGP) but its role in TGP pathogenesis remains unclear. The aim of this study was to evaluate the significance of GL in TGP.

Design: Renal transplant biopsies with TGP (n=50) and indication transplant biopsies without TGP (n=46, control) were retrospectively reviewed. GL was defined on light microscopy (LM) by the presence of monocytes or neutrophils affecting > 30% of glomeruli. TGP was defined by LM as mesangioproliferative glomerulonephritis and by EM with the following: endothelial fenestrae closure, subendothelial expansion, glomerular basement membrane (GBM) duplication, GBM multi-lamination, and luminal inflammatory cells. These EM features were scored as follows: 0 none; 1 <25% of capillary loops affected; 2 26-50% and 3 >50%. Laboratory data included urine protein. Statistical analysis using a t test was used to correlate GL, TGP and GBM multi-lamination with proteinuria.

Results: 10/50 (20%) cases of TGP showed GL compared with 1/46 (2%) control transplant biopsies. Neutrophils were a significant component of GL in 9/10 cases. EM was available for 43 cases (8 TGP with GL, 17 TGP, and 18 controls). The g score for TGP and TGP with GL was similar (1.8); 5/8 TGP cases with GL showed GBM multi-lamination. However, TGP with GL showed focal multi-lamination (score=1), whereas TGP without GL had a broad range of multi-lamination (score=0-3). There was a trend towards increased proteinuria associated with GL (3.35 g/day vs. 2.08 g/day). There was a stronger correlation of GBM multi-lamination with proteinuria (4.25 g/day vs. 2.35 g/day; p=0.08). 2/10 (20%) cases of TGP with GL showed peritubular capillary C4d staining compared with 12/25 (48%) cases of TGP without GL. The GBM multi-lamination score tended to correlate with C4d staining in PTC (1.2 versus 0.8).

Conclusions: Our results suggest a key role for neutrophils in the pathogenesis of GBM injury in TGP. We propose that neutrophils may mediate development of GBM multi-lamination in established TGP. A correlation of multi-lamination with C4d peritubular capillary immunoreactivity is consistent with the concept that both are features of chronic transplant capillaropathy.

1462 Dystroglycan Patterns in FSGS Variants.

G Giannico, S Phillips, Y Shyr, CE Alpers, VD D'Agati, AB Fogo. Vanderbilt University, Nashville, TN; University of Washington, Seattle; Columbia University, New York, NY.

Background: Background: The dystroglycan (DG) glycoprotein complex links podocytes to the glomerular basement membrane, and through interaction with utrophin interacts with actin in the cytoskeleton. Decreases in αDG have been variably reported in minimal change disease (MCD). αDG contains sialic acid, a necessary component for maintenance of foot processes and the filtration barrier. We investigated whether αDG was altered in variants of FSGS, classified according to the Columbia Classification.

Design: 69 biopsies (5 cellular, 17 collapsing, 3 perihilar, 18 tip, 19 NOS, 7 MCD) with a total of 1289 glomeruli were investigated. Each glomerulus was scored for αDG (0-3 intensity) in the lesional and non-lesional segments in involved glomeruli and in uninvolved glomeruli without segmental lesions.

Results: A mix of lesions were present in biopsies, with 39 glomeruli with cellular lesions, 401 with collapsing lesions, 296 with NOS lesions, 45 with perihilar lesions and 329 with tip lesions. αDG staining was decreased in uninvolved glomeruli in NOS (intensity 2.75), tip (2.79) and minimally decreased in cellular variant cases (2.86), with least staining in uninvolved glomeruli in collapsing glomerulopathy (intensity

2.60). Uninvolved glomeruli showed unaltered αDG in biopsies with perihilar FSGS and in MCD (3.00). Segmental lesions showed nearly absent staining in collapsing glomerulopathy (0.12), with similar low level staining in NOS lesions, and slightly more staining in tip lesional areas (1.00).
Conclusions: αDG staining is decreased in lesional areas of segmental sclerosis, and particularly decreased even in uninvolved segments of glomeruli in collapsing glomerulopathy. We speculate that this may reflect dedifferentiation of podocytes. Furthermore, these findings indicate that decreased dystroglycan may not be specifically or uniquely related to the podocyte perturbations underlying minimal change disease.

1463 Early Ultrastructural Abnormalities of Transplant Glomerulopathy (TG): Correlation with C4d-Positive and C4d-Negative Antibody-Mediated Rejection (AMR) and Subsequent Development of Overt TG.

M Haas. Cedars-Sinai Medical Center, Los Angeles, CA.
Background: TG is correlated with reduced renal allograft survival and with donor-specific antibodies (DSA). Overt TG, with double contours of the glomerular basement membrane (GBM) on PAS and silver stains, is typically seen >1 year post-transplantation (PT). However, electron microscopic (EM) changes correlated with development of overt TG may be seen much earlier; these include glomerular endothelial swelling, subendothelial electron-lucent widening, and early GBM duplication [Wavamunno et al, AJT 7: 1-12, 2007]. This study aims to examine the specificity of these early EM changes for AMR, both C4d-positive and C4d-negative, and determine if these are inevitably associated with later development of overt TG.
Design: From 1/07 – 12/09, 119 renal allograft biopsies were done within the first 3 months PT on patients followed at our center; of these 95 (from 91 patients) were examined by EM. The remaining 24 had inadequate tissue for EM or were repeat biopsies. The 95 biopsies form the study group; indirect immunofluorescence for C4d was done on all 95, and DSA data at the time of biopsy was available for 69.
Results: Of the 95 biopsies, 12 showed C4d+ AMR with glomerulitis and/or peritubular capillaritis (Banff g + ptc ≥2), peritubular capillary C4d (diffuse in 11), and DSA; 2 also had Banff type 1 cellular rejection (ACR). 7 biopsies showed histologic changes of AMR with DSA, but no C4d (C4d- AMR); 4 had type 1 ACR. 21 additional biopsies had type 1 (16) or type 2 (5) ACR; 55 had no diagnostic rejection. One or more early EM changes of TG were seen in 12/12 biopsies with C4d+ AMR, 6/7 with C4d- AMR, 8/21 with ACR (2 with histologic changes of AMR, but no DSA data), and 6/55 with no rejection. All 3 early EM changes of TG were seen in 7/12, 4/7, 3/21, and 0/55 biopsies, respectively. 14 patients (including 5 with C4d+ AMR and 4 with C4d- AMR) with ≥1 early EM changes had ≥1 follow-up biopsy 3.5 – 19 months PT. Of these 5/8 patients with persistent histologic changes of AMR and 0/6 without developed overt TG. All 5 patients with C4d+ AMR were treated for AMR and 1 developed overt TG; by contrast 0/4 patients with C4d- AMR were initially treated for AMR and 3/4 developed overt TG.
Conclusions: Early EM changes of TG are seen in most cases of C4d+ and C4d- AMR and are often associated with development of overt TG, especially if there are presistent histologic changes of AMR. However, this progression does not appear to be inevitable, at least during the first 2 years PT.

1464 Distinct Histopathologic Changes Elicited in Baboon Kidneys after Challenge with Shiga Toxin Type 1 or 2 from Enterohemorrhagic E. coli.

JM Henderson, S Kurosawa, DJ Stearns-Kurosawa. Boston University Medical Center, MA.
Background: Shiga toxin-producing E. coli (STEC) are an important cause of regional outbreaks of acute hemorrhagic enteritis and hemolytic uremic syndrome. Long-term renal impairment is often a consequence of STEC infection. STEC may produce either or both of two virulent toxins, Stx1 and Stx2, which share similar structure and cell receptors. Despite similarities, STEC producing primarily Stx2 is more often associated with kidney injury in patients, and the mechanism is not known. We investigated effects of each Shiga-like toxin on kidneys in a baboon model.
Design: Anesthetized juvenile baboons (*Papio*) were challenged with an i.v. toxin dose (Stx1:10, 50, 100 ng/kg; Stx2: 10, 50 ng/kg), and followed until euthanasia was performed up to seven days post challenge. Necropsy kidney tissue was processed for standard renal histopathologic examination.
Results: Kidneys from Stx2-challenged animals showed the most severe changes. High dose Stx2 (n=6; 50 ng/kg, euthanasia <128hrs) elicited severe changes including interstitial hemorrhage (most prominent in the medulla), prominent tubulointerstitial injury and polymorphonuclear inflammation, and striking apoptotic changes in glomerular mesangial cells. Glomerular capillary wall changes (thickening, double contours) were overall mild and focal with high-dose Stx2. In contrast, higher dose Stx1 (n=10; 50, 100ng/kg; euthanasia <74hrs) resulted in more substantial glomerular capillary wall changes (moderate thickening and double contouring) along with moderate tubular injury. Mesangial apoptotic changes were not seen in Stx1-challenged animals. Low dose Stx2 (n=4; 10ng/kg) and low dose Stx1 (n=3; 10ng/kg) showed minor or no significant changes, respectively.
Conclusions: Overall kidney injury was more severe after Stx2 challenge, although euthanasia was required earlier in Stx1 animals, possibly obscuring further Stx1-mediated damage with time. The pattern of glomerular injury with Stx1 challenge featured prominent "HUS-like" capillary wall changes, whereas that with Stx2 challenge was predominantly characterized by mesangial cell apoptotic changes. Thus, Stx1 and Stx2 had distinct effects on the glomerulus, with endothelial injury predominating with Stx1 and mesangial injury predominating with Stx2. The novel finding of Stx2-induced mesangial cell injury raises new avenues of investigation into mechanisms of renal damage after STEC infection.

1465 Acute Renal Failure in Cocaine Users: Pathology Correlates.

GA Herrera, EA Turbat-Herrera. Nephrocor, Tempe, AZ.
Background: A subset of patients using cocaine develop acute renal failure. Most of these patients do not volunteer the information that they have used cocaine in the immediate period prior to the development of renal failure. The mechanisms involved appear to be multifactorial and involve vasoconstriction with tubular injury and direct effect of the cocaine on proximal tubules where it is normally metabolized, as well as a possible hypersensitivy reaction to either cocaine itself or to other products admixed with it.
Design: A review of 2376 renal biopsies over a 4 year period revealed 12 cases with cocaine-related acute renal failure. The study is carried out to identify the histopathological, ultrastructural, and immunohistochemical findings associated with this entity.
Results: An antibody to cocaine metabolites identified the presence of these in proximal tubular cells in all cases. The pathology identified included acute tubular injury and a generally subdued interstitial inflammatory process associated with tubulitis and tubular damage. The inflammatory cells were predominantly lymphocytes and plasma cells, but eosinophils were present in most cases, albeit in variable numbers. By immunohistochemistry cocaine metabolites are identified in the cytoplasm of proximal tubular cells. Ultrastructurally, the damaged proximal tubules reveal large secondary lysosomes with particulate matter inside, a rather typical marker.
Conclusions: Identifying cases of cocaine-related acute renal failure requires a high index of suspicion as the pathologic findings are rather non-specific and often, quite focal and unimpressive. Ultrastructural evaluation is helpful to detect specific changes in damaged proximal tubular cells suggestive of recent cocaine use. This is very helpful to suggest a possible cocaine etiology for the tubular damage and may lead to the request for immunohistochemistry for cocaine metabolites. Immunohistochemistry stain for cocaine metabolites may provide a reliable marker to identify these cases.

1466 Cross-Species Identification of Conserved Glomerular Transcriptional Networks of Progressive Diabetic Nephropathy in Mouse and Man.

JB Hodgin, V Nair, H Zhang, A Randolph, RC Harris, RG Nelson, FC Brosius, M Kretzler. University of Michigan, Ann Arbor; Vanderbilt University, Nashville, TN; NIDDK, Phoenix, AZ.
Background: Mouse models of diabetic nephropathy (DN) are valuable tools, but no mouse model reliably exhibits all features of human disease, hindering our ability to identify specific factors that cause or predict DN. To define where mouse models of diabetic glomerulopathy (DG) faithfully recapitulate human DG on a functional level using a cross-species comparison to identify shared transcriptional networks.
Design: Transcriptional networks for diabetic humans and AMDCC mouse models were generated using glomerular mRNA, Affymetrix microarrays, transcriptional pathway mapping, and promoter modeling tools. The human transcriptional network was derived from albuminuric (>30 mg/g Alb/Cr) versus nonalbuminuric (<30 mg/g Alb/Cr) Pima Indians, a cohort with early, progressive DG, and from later stage diabetics versus living donor controls. Mouse transcriptional networks were derived from streptozotocin treated DBA/2 mice, db/db C57BLKS mice, and eNOS-deficient db/db C57BLKS mice, each versus control.
Results: Integrating the gene expression alterations with biological knowledge resulted in complex networks of 1000s of genes linked by multiple co-citations and promoter binding sites (Genomatix Bibliosphere). TALE (Tool for Approximate Large Graph Matching, University of Michigan) was used to align the human and mouse transcriptional networks to derive three conserved network structures for each human-mouse comparison, comprised of approximately 100 nodes representing key hubs of conserved regulatory events. Shared gene nodes were found in all three networks, many of them reflecting established pathogenetic mechanisms of diabetic complications including JAK-STAT, VEGF, c-kit, and HGF-R signaling pathways. Shared top biological processes included cytokine mediated signaling, response to steroid hormone, and JAK-STAT cascade.
Conclusions: Comparing TALE networks from early progressive DG (PIMA albuminuric versus nonalbuminuric) against established DG (albuminuric diabetics versus nondiabetics) revealed pathways specific to glomerular disease progression. This approach can guide the selection of disease pathways in mouse models that are the most relevant to the human disease process and identify new pathways that are excellent targets for future study.

1467 Quantitation of IgG4+ Plasma Cells in Tubulointerstitial Nephritis.

DC Houghton, ML Troxell. Oregon Health and Sciences University, Portland.
Background: IgG4-related tubulointerstitial nephritis (IRTIN) is a sclerosing lymphoplasmacytic inflammatory disorder that may affect the kidney alone, or may be part of the multi-system disorder, IgG4-related systemic disease (IRSD). Auto-immune pancreatitis (AIP) is the most common lesion of IRSD. The active inflammatory lesion in IRTIN is characterized by the presence of numerous IgG4+ plasma cells (IgG4+PC), but the specificity of this finding has not been determined. In this study we investigated the prevalence of IgG4+PC in renal interstitial infiltrates.
Design: We examined all renal biopsy samples with active interstitial inflammation, regardless of principal diagnosis, from 1/1/09 through 6/1/10, to determine the presence and extent of IgG4+PC in the infiltrates (N=100). Two observers independently scored each case for the density and extent of infiltrates, the apparent proportion of plasma cells, the extent and density of CD138+ plasma cells, and the distribution and numbers of IgG4+PC in the infiltrate.

Results: 29 cases were negative for IgG4+PC and 63 had fewer than 2 per high power field (hpf). The highest numbers of IgG4+PC were seen in some cases of diabetic nephropathy (DN), idiopathic interstitial nephritis (IISN), diffuse lupus nephritis (DLN), membranous glomerulonephritis (MGN), and necrotizing glomerulonephritis (NGN), including pauci-immune lesions, and those with granular and linear immune deposits:

Table 1

Diagnosis	# of IgG4+PC/hpf				
	0-2	3-5	6-10	11-20	20-120
DN	3		3	2	
IISN	3	2		1	1
DLN	5				1
MGN	4	3		1	
NGN	8	3	1	1	4

# of cases in diagnosis categories with numerous IgG4+PC

Three biopsies from patients with Sjogren's syndrome demonstrated 0.7, 2.5 and 3.0 IgG4+PC/hpf, and a biopsy in the setting of tubulointerstitial nephritis-uveitis syndrome (TINU) was negative for IgG4+PC. PC were prominent in all cases with more than 20 IgG4+PC. The numbers of IgG4+PC did not correlate with severity of fibrosis, or the presence or absence of eosinophils. By comparison, infiltrates in a 2005 biopsy of IRTIN demonstrated dense sclerosis and numerous eosinophils, and contained more than 200 IgG4+PC/hpf.

Conclusions: Infiltrates of numerous IgG4+PC's are rare in renal biopsies, regardless of the density and activity of the inflammation, but they may be seen in some non-IRTIN cases, particularly in NGN. It may be instructive to further investigate our cases with this finding: in MGN because of it's known association with IRTIN; in DN because it may develop as a complication of AIP; and in IISN to rule out previously unsuspected IRTIN.

1468 C4d/CD34 Co-Immunofluorescence Staining for the Evaluation of the Extent of C4d Positivity in Renal Transplants.

K-Y Jen, TB Nguyen, ZG Laszik. University of California San Francisco.

Background: Immunofluorescence (IF) detection of the complement split product C4d along tubulointerstitial (TIS) capillaries of transplant kidney biopsies is the mainstay of diagnosing antibody-mediated rejection (AMR). The extent of C4d positivity may have significant clinical ramifications; however, precise quantitative assessment of the proportion of TIS capillaries that are C4d-positive is often difficult, if not impossible. The aim of our study is to develop a C4d/CD34 double IF stain that allows not only rapid and sensitive detection of C4d positivity, but also precise and reproducible morphometric quantitation of the fraction of C4d-positive TIS capillaries.

Design: Renal transplant biopsies with C4d-positive acute or chronic AMR (n=10) as determined by single IF staining for C4d on frozen sections were used for the study. Two biopsies negative for C4d IF were used as negative controls. Frozen sections were stained with a mixture of polyclonal rabbit anti-C4d (ALPCO) and mouse anti-CD34 (Dako) antibodies followed by incubation with a mixture of fluorescein isothiocyanate (FITC)-labeled goat anti-rabbit (Vector) and Texas Red-labeled horse anti-mouse (Vector) antibodies. Digital photographs of multiple fields were taken from each double-stained slide at 20x magnification for FITC and Texas Red IF. The photographs were processed using Just Another Colocalization Plugin (JACoP) for the ImageJ® software in order to calculate the extent of colocalization of C4d and CD34 positivity in the TIS capillaries. Manders coefficients M1 and M2 were used to determine the extent of colocalized staining. To assess the sensitivity of the C4d/CD34 double IF stain for C4d detection, the findings of C4d positivity in the double-stained sections were visually compared to the corresponding fields of serially-cut frozen sections stained for C4d alone.

Results: The extent and intensity of the C4d positivity was comparable in the double (C4d/CD34) and single (C4d) IF-stained sections. Colocalization of C4d and CD34 in the TIS capillaries as assessed by Manders coefficient M2 ranged from 0.17 to 0.87. A high degree of correlation was observed between various fields in the same biopsy for the extent of colocalization of C4d and CD34 positivity.

Conclusions: C4d/CD34 double IF stain on frozen sections yields rapid and sensitive detection of TIS capillary C4d positivity in renal transplant biopsies. It also allows simple, precise, and reproducible morphometric determination of the C4d-positive fraction of the CD34-positive TIS capillaries.

1469 IGG Subclass Staining in Allograft Membranous Nephropathy.

N Kearney, J Podolak, D Houghton, M Troxell. OHSU, Portland, OR.

Background: Membranous glomerulopathy (MGN) recurs in the renal allograft 10-50% of the time, but may also occur de novo in about 2% of all grafts. The mechanisms of glomerular injury in recurrent and de novo MGN are likely to be different, possibly analogous to the difference between "idiopathic" and secondary MGN in native kidneys, including different profiles of IgG subclasses in the immune deposits. IgG4 in subepithelial deposits is generally associated with "idiopathic" MGN, and was recently shown to have specificity for PLA2R on podocytes in most patients. Differential deposition, with a predominance of IgG1, IgG2 or IgG3, has been found in native kidneys with secondary MGN, associated with malignancy, lupus, and probably infection. Our study examines the IgG subclass distributions in MGN in allograft kidneys.

Design: Department of Pathology files were searched for allograft kidneys with MGN from 2003-2010 with available frozen tissue containing glomeruli. Specimens from 10 patients were identified, ranging in age from 8-75. No patient had a known malignancy, Hepatitis B or C. Of these, 6 were apparently recurrent MGN, and 4 were de novo MGN. Frozen sections were immunofluorescently stained with antibodies to IgG1, IgG2, IgG3, IgG4 (The Binding Site), and examined under UV light. Granular capillary loop immunofluorescence was scored independently on a scale of 0-3+ by 3 observers blinded to clinical history.

Results: IgG4 was dominant or co-dominant IgG subclass in the capillary loop deposits in all 6 cases of recurrent MGN. In contrast, IgG4 was not dominant in any of the 4 cases of de novo MGN (0/4), with generally weak staining. Instead, IgG1 staining was strongest in 3 of 4 de novo MGN cases; IgG1 and IgG3 were co-dominant in the fourth case, in a young boy transplanted for obstructive uropathy. The average intensity of IgG1 staining was comparable across the recurrent and de novo MGN groups (1.75), while the average IgG4 staining score was higher in recurrent (2.1) as compared to de novo MGN (1.0).

Conclusions: Our cases demonstrate dominance or co-dominance of IgG4 in capillary loop immune deposits in recurrent MGN, as reported in "idiopathic" MGN in native kidneys. In contrast, cases of de novo MGN in allografts demonstrate a different IgG subclass profile, with dominance of IgG1 or IgG3, and generally less IgG4. IgG subclass staining these cases provides further evidence of different pathophysiologies of recurrent and de novo MGN in renal allografts. Further studies are indicated to confirm these findings, to better establish their diagnostic importance, and to correlate them with PLA2R antibody assays, as they become available.

1470 Renal Amyloidosis and Clinicopathological Prognostic Factors: A Study of 196 Cases.

K Kosemehmetoglu, D Baydar. Hacettepe University Hospital, Ankara, Turkey.

Background: In this study, we aimed to analyze our cases of renal amyloidosis diagnosed by needle biopsy and document their clinical and morphological features.

Design: Biopsy slides were retrieved from the archives and reviewed. Intensity and relative distribution of amyloid deposition in renal compartments were noted. Glomerular deposits were classified as hilar, mesangial segmental, mesangial nodular and mesangiocapillary. Chronic tubulointerstitial damage was graded from 1 to 3 according to its extent (<25%, 25-75% and >75%). Amyloid typing was performed by immunohistochemistry using anti-AA, lambda, kappa, apolipoprotein A, prealbumin (transthyretin), fibrinogen and lysosyme antibodies. Clinical information and follow-up data were gathered from hospital records and computer-based patient data system.

Results: Between years from 1981 to 2006, we found 196 needle biopsies with renal amyloidosis. Immunohistochemical studies could be achieved in 178 cases. Among them 168 were AA type, 3 were AL type and 1 was AFib, AApoA1 and ALys for each; 4 cases were unable to be categorized immunohistochemically. Within AA amyloidosis group, the most common preamyloidotic disease was Familial Mediterranean Fever (FMF) (29%), followed by chronic infectious diseases (tuberculosis-%16, bronchiectasis-%8) and chronic inflammatory conditions (rheumatoid arthritis-%9, Behcet's disease-%7). Patients almost always presented with edema due to proteinuria. 18% of patients had disturbed renal fuction at the time of diagnosis. Hypertension was recorded in 32% and hematuria in 45%. Glomerular amyloid deposition was noted to fall into 4 distinct patterns: Mesangial segmental (15.5%), mesangial nodular (11.3%), hilar (30.4%) and mesangiocapillary (42.8%). Regarding the compartment of dominant amyloid deposition, cases were further classified as glomerular-dominant (28.1%), vascular-dominant (15.8%) and co-dominant (51.5%) forms. Glomerular-dominant form closely correlated with level of proteinuria (p=0.008) and presence of hypertension (p=0.009). 5- and 10-year survivals were 37% and 30%, respectively. In multivariant analysis, the poor prognostic factors determining renal survival were low glomerular filtration rate and high 24-hr urine protein, mesangiocapillary type glomerular amyloid deposition and high renal injury score at the time of biopsy.

Conclusions: AA is the most common amiloid type seen in renal biopsies in our country in which FMF is endemic. Renal amyloidosis has a diverse pathology in terms of preferential location of amyloid deposition and its intensity. Patients follow variable clinical courses accordingly.

1471 Clinical Significance of Isolated Arteritis (Banff Class 2A) in the Post-Transplant Period. A Single Institution Review.

M Kuperman, LJ Arend, S Bagnasco, L Racusen, M Haas, E Kraus. Johns Hopkins Medical Center, Baltimore, MD; Cedars Sinai Medical Center, Los Angeles, CA.

Background: Infiltration of mononuclear cells beneath the endothelial cells of arteries/arterioles is considered pathognomonic of acute cell-mediated rejection (ACR). However, it was recently shown that some biopsies diagnosed with ACR based solely on intimal arteritis (V1) do not have molecular features of rejection (Famulski, AJT 2010). We retrospectively examined renal transplant biopsies with isolated V1 lesions (minimal interstitial inflammation and tubulitis) to see how many continued to show ACR on follow-up.

Design: The patient cohort consisted of recipients of kidney transplants at Johns Hopkins Hospital from January, 2000 – June, 2009; ABO incompatible and cross-match incompatible grafts were excluded. Both for-cause and protocol biopsies were included. All C4d-negative biopsies that met Banff criteria of v=1, t<2, i<2 were collected for further study. Follow-up biopsies for each case were also examined; cases with no later biopsies were excluded.

Results: 49 cases of isolated V1 were collected; 16 were excluded due to the lack of follow-up biopsies. Of the remaining 33 cases, 23 (70%) were in deceased donor grafts. ACR on follow up biopsies was found in 4/8 (50%) isolated V1 lesions occurring during the first week, 0/6 V1 occurring from day 8-14, and 16/19 (84%) V1 occurring after week 2. Of 4 biopsies done from day 3-6 for increased serum creatinine (SCr) 3 had ACR type 1B or 2B on follow-up; only 1/5 early (day 3-14) biopsies done for delayed graft function (DGF) and 0/5 early protocol biopsies showed ACR on the follow-up biopsy.

Significance of Isolated V1 Lesions in first 2 weeks

Days 1-7	Biopsy Reason	Last Bx Result
3 days	↑Creatinine	Grade 1B
3 days	↑Creatinine	Grade 2B
5 days	↑Creatinine	No rejection
5 days	DGF	Grade 2C
6 days	↑Creatinine	Grade 2B
6 days	Surveillance	No rejection
7 days	Surveillance	No rejection
7 days	DGF	No rejection
Days 8-14		
8 days	Surveillance	No rejection
10 days	DGF	No rejection
10 days	DGF	No rejection
12 days	Surveillance	No rejection
13 days	DGF	No rejection
14 days	↑Creatinine	No rejection

Conclusions: Isolated V1 lesions found on early biopsies done for increased SCr and on later biopsies usually represent ACR. By contrast, such lesions found on early protocol biopsies and biopsies done for DGF are rarely associated with continued ACR on follow-up. To further investigate these findings, a multicenter study of isolated V1 lesions is currently underway.

1472 Glomerular Endothelial Injury in Patients with Non-Renal Transplants: Are We Missing Subclinical Thrombotic Microangiopathy?

YB Kushner, FA Malik, AB Collins, RK Holmes, RN Smith, RB Colvin. Massachusetts General Hospital, Boston.

Background: Approximately 20% of recipients of heart, liver, lung or bone marrow transplants develop chronic renal failure. This study aimed to elucidate the value of the renal biopsy, the contribution of thrombotic microangiopathy (TMA) and a novel means to assess glomerular endothelial damage.

Design: An institutional database containing 9,729 renal biopsies identified 32 patients with non-renal transplants (heart, lung, liver, and bone marrow). Clinicopathologic parameters were extracted and biopsies were reviewed by a pathologist. Ultrastructural signs of glomerular endothelial damage were assessed using a novel scoring system. The degree of endothelial fenestration was measured in 5-10 glomerular capillary loops; 10 patients with minimal change disease (MCD) were scored for comparison.

Results: The median patient age was 49 (range 20-74). Median time from transplant to renal biopsy was 42 months (range 1-168). The renal diagnoses were: 19 focal segmental glomerulosclerosis (FSGS), including 5 with features of collapsing FSGS; 9 TMA; 4 immune complex glomerulonephritis, including 2 with HCV-related disease and one with IgA nephropathy; 25 with arteriolar hyalinosis; and 20 with more than 25% interstitial fibrosis (many had more than one diagnosis). The mean serum creatinine at the time of biopsy was 3.7 (+/-1.9). Median platelet count was 169,000/mm2 (+/-70,000). Glomeruli had fewer endothelial fenestrations compared with controls with MCD (45 +/-31% vs 89 +/-7%, respectively; $p<0.001$). Loss of endothelial fenestrations was present in 77% of the biopsies, including 75% of the patients with collapsing FSGS. The percent of endothelial area with fenestrations was correlated with the platelet count ($p<0.05$), even though most of the patients did not have diagnostic signs of TMA. 18 patients progressed to end-stage renal disease (ESRD) and/or required renal transplantation.

Conclusions: Patients with non-renal transplants frequently develop renal failure, which in this series was biopsied late in the course. TMA, likely related to calcineurin inhibitors, has been associated with poor renal survival in these patients. Glomerular endothelial injury is known to be a feature of TMA, and, as assessed by our novel scoring system using ultrastructural findings, may allow detection of subclinical TMA in the absence of typical clinical or light microscopic features. Patients with subclinical TMA may benefit from modified treatment modalities to reduce their risk of progression to ESRD.

1473 Isolated Light Chain Proximal Tubulopathy without Crystal Formation – An Under-Recognized and Critically Important Entity.

CP Larsen, PD Walker. Nephropathology Associates, Little Rock, AR.

Background: The renal diseases most frequently associated with myeloma include light chain deposition disease, cast nephropathy, and amyloidosis. Less frequently reported is light chain proximal tubulopathy (LCPT) characterized by kappa-restricted crystal deposits in the proximal tubule cytoplasm. These patients classically present with Fanconi syndrome in the setting of smoldering myeloma. LCPT without crystal deposition is only loosely related to the typical LCPT. Little is known about this entity as only 3 cases have previously been reported compared with over 50 cases of LCPT with crystals. We describe 10 cases of LCPT without intra-cytoplasmic crystals and detail the pathologic and clinical significance of this not so uncommon condition.

Design: A search was performed of the 10081 native kidney biopsies processed by our laboratory over the past 2 years for cases that had light chain restriction limited to the proximal tubule cytoplasm by immunofluorescence without evidence of other concurrent paraproteinemic renal diseases on biopsy. All cases were evaluated by light, immunofluorescence, and electron microscopy.

Results: 13 cases of isolated LCPT were found representing 4.0% of light chain-related diseases. 10/13 cases of LCPT did not have intracytoplasmic crystals and 9 of these 10 showed lambda restriction. In the cases with crystals, 2 were kappa subtype. Only 3/10 patients with LCPT without crystals had a diagnosis of a plasma cell dyscrasia at the time of renal biopsy. After the biopsy was reported, follow-up was available on 9/10 patients with 9/9 showing a plasma cell dyscrasia. 8/9 had multiple myeloma, only one of which was classified as smoldering myeloma. Six of the patients without crystals were tested for Fanconi'syndrome and none were positive.

Conclusions: LCPT without crystal formation is a diagnostic entity on renal biopsy that has several distinctions from the more commonly described LCPT with crystals. Whereas, over 90% of cases with crystals in the literature are of the kappa subtype, our series shows that 90% without crystals are of the lambda subtype. Additionally, PLCT without crystals is more likely to be associated with multiple myeloma than PLCT with crystals and less likely to be associated with a Fanconi syndrome. The fact that LCPT without crystals is so rarely described in the medical literature despite being more than 3 times as prevalent in our series leads us to believe that it is an under recognized entity. And given that it is often associated with previously unrecognized myeloma, it is a critically important diagnosis.

1474 Validation Study of Oxford Classification of IgA Nephropathy in a Chinese Cohort.

S Liang, C Zeng, S Phillips, Y Shyr, S Troyanov, Z-H Liu, AB Fogo. Nanjing Research Institute of Nephrology, Jiangsu, China; Vanderbilt Unversity, Nashville, TN; Hôpital du Sacré-Coeur de Montréal, University of Montreal, QC, Canada.

Background: The Oxford Classification of IgA Nephropathy (IgAN) identified four renal biopsy lesions of prognostic significance, namely mesangial hypercellularity, segmental glomerulosclerosis/adhesion, endocapillary proliferation and significant tubular atrophy/interstitial fibrosis. We now sought to validate whether these results were applicable in a Chinese cohort of patients.

Design: 213 adult Chinese patients from a single center, Nanjing Research Institute of Nephrology were studied. Inclusion criteria were as in the original Oxford cohort, with eGFR ≥ 30 ml/min and minimum of one year follow up, excluding patients with rapid progression in less than a year, or with no or minimal proteinuria, diabetes or other glomerulonephritis. Renal biopsies included at least 10 glomeruli.

Results: Patients were on average age 34 years (range 18-65), 46.5% female. MAP was higher than in the Oxford cohort (102 ± 22 mm Hg) at time of biopsy. RAS blockade at time of biopsy, and during followup were similar to the Oxford cohort. Follow up was on average 81 months (range 30-157 months). 21.1% received immunosuppression, 14.6% prednisone and 7.5% cyclophosphamide, all slightly less than the Oxford cohort. Rate of renal function decline was -2.2 ± 4.2 ml/min per 1.73 m^2 per year, with 20.2% reaching 50% decline in renal function and 14.1% reaching ESRD, all similar to the original Oxford cohort. On average, 22.7 ± 8.8 (range 8-61) glomeruli were available. All Oxford classification variables were scored independently by two pathologists. Global sclerosis/advanced segmental sclerosis was present in 19.8% of glomeruli. Segmental sclerosis was present in 85% of biopsies. Significant mesangial hypercellularity, endocapillary proliferation, segmental sclerosis were present in, on average, 65, 22 and 85% of biopsies. Significant tubulointerstitial fibrosis (T1 or T2), >25%, was present in 33%. Tubulointerstitial fibrosis correlated with proteinuria and loss of eGFR over time, and endocapillary proliferation (E1) correlated with proteinuria over followup. Mesangial proliferation (M1) and segmental sclerosis/adhesion (S1) did not predict changes in eGFR or proteinuria in this cohort.

Conclusions: In conclusion, application of the Oxford IgAN classification to Chinese patients shows similar trends for prediction of clinical outcome in some, but not all variables, as the previous data set.

1475 Application of the Columbia Classification of Focal Segmental Glomerulosclerosis in Kidney Biopsies from Patients with HIV Infection.

SM Meehan, L Kim, A Chang. University of Chicago, IL.

Background: The Columbia system of classification of focal segmental glomerulosclerosis (FSGS) identifies 5 different types or variants of this distinct glomerular lesion. FSGS of the collapsing variant is a classical feature of HIV associated nephropathy. Other variants of FSGS have also been described in this disorder. We examined the spectrum of FSGS lesions in biopsies obtained from patients with HIV infection using the Columbia classification system.

Design: We identified 43 renal biopsies from 42 patients with HIV infection obtained over a 7 year period. Twenty five biopsies had FSGS. Reproducibility of the Columbia system was good (kappa 0.65).

Results: Sixteen biopsies had FSGS, collapsing variant (coll) (64%). Six had FSGS not otherwise specified (NOS) (24%). Fifteen biopsies (60%) had focal glomerular capillary collapse without visceral epithelial hyperplasia (10 coll, 4 NOS, 1 cell). One each had cellular (cell), tip lesion (T) and perihilar (Ph) variants. Glomeruli with features of multiple variants of FSGS were frequently identified in the same biopsy and included coll with NOS (n=9), cell (n=5), or Ph (n=3), cell and NOS (n=1), T and NOS (n=1).

Conclusions: It is no surprise that collapsing FSGS was the commonest variant observed in biopsies from HIV infected patients. NOS lesions were less common and other variants rare. Mixed Columbia FSGS lesions were evident in more than half of this sample (52%). Mixed patterns of FSGS raise the possibility that Columbia FSGS variant lesions may form part of a spectrum of glomerular responses to injury in HIV infection.

1476 Deficiency of B Cells but Not Mast Cells Ameliorates Chronic Allograft Damage in a Mouse Model for Renal Transplantation.

M Mengel, K Famulski, J Chan, L Hidalgo, B Sis, P Halloran. University of Alberta, Edmonton, Canada.

Background: We recently observed that the number of B cells and mast cells increases with time post transplantation in human renal allografts. Furthermore these two cell types predominately accumulate in areas of interstitial fibrosis and tubular atrophy (IFTA), suggesting a potential pathogenetic role of these cell in the onset and/or progression of IFTA.

Design: We analyzed the long-term time course of transplanting a wild type allograft (CBA) into a B cell (B6.129S2-Igh-$6^{-/-}$) or mast cell (C57BL/6-KitW-v/W-v) deficient recipient and compared the findings to respective controls (CBA into B6 wild type). This strain combination (CBA into B6) represents transplantation across complete MHC incompatibility. Transplants were done in a non-life supporting model without

any treatment and thus developed the natural course of rejection. Transplanted kidneys were harvested on day 7, 14, 21, 42, and 60 (total n=150) and analyzed by histopathology according to Banff criteria.

Results: B cell deficient recipients: At early time points (day 7 and 14) no significant differences in terms of interstitial infiltrates were found between controls and deficient recipients. On day 7, B cell deficient recipients showed significantly more tubulitis (p=0.004), but on day 21 a trend towards less interstitial inflammation and tubulitis. From day 42 and persisting to day 60, B cell deficient recipients showed significantly less, only focally present interstitial infiltrates and tubulitis. This resulted in significantly less interstitial fibrosis on day 60.

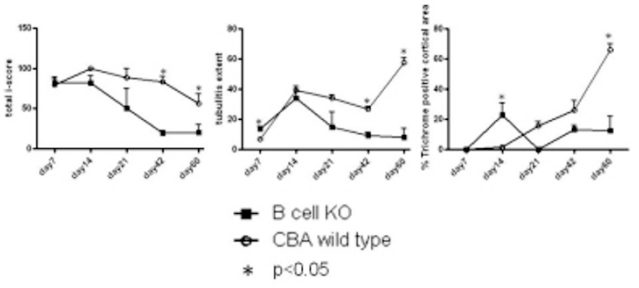

Mast cell deficient recipients: On day 7 and day 14 the deficient recipients showed significantly more interstitial fibrosis compared to controls. More mast cell deficient mice showed extensive necrosis and arterial thrombosis at late time points of harvest, i.e. day 42 and day 60.

Conclusions: Absence of B cells in the recipient has no influence on early cellular rejection of mice renal allografts. In contrast long-term maintenance of the inflammatory response and thus onset of chronic injury is dependent on the presence of B cells. In contrast mast cell deficient recipients show more vigorous acute rejection, potentially indicating an immune-modulatory role for this cell type.

1477 The Molecular Phenotype of Six-Week Protocol Biopsies from Human Renal Allografts: Reflections of Prior Injury but Not Future Course.

M Mengel, J Chang, D Kayser, W Gwinner, A Schwarz, G Einecke, V Broecker, K Famulski, D De Freitas, L Hidalgo, H Haller, B Sis, P Halloran. University of Alberta, Edmonton, Canada; Hannover Medical School, Germany.

Background: Protocol biopsies after renal transplantation are considered a surveillance tool for detection of subclinical pathologies at a stage where they are potentially more amenable to therapy.

Design: We assessed the molecular phenotype of 107 six-week protocol biopsies from human renal allografts, using Affymetrix microarrays. Transcript changes were summarized as pathogenesis-based transcript sets (PBTs) reflecting inflammation (T cells, macrophages, IFNG effects) and the injury-repair response of the parenchyma, stroma, and microcirculation – increased ("injury-up") and decreased ("injury-down") transcripts.

Results: The molecular changes were highly correlated with each other, even when all rejection and borderline cases were excluded. Inflammation and injury-down PBTs correlated with histologic inflammation and tubulitis, and the inflammation transcripts were greater in kidneys diagnosed as T cell-mediated or borderline rejection. In terms of their molecular phenotype no difference between borderline and T cell mediated rejection was found (figure 1a). Injury-up PBTs did not correlate with histopathology but did correlate with kidney function: thus functional disturbances are represented in transcript changes but not in histopathology. PBT changes correlated with prior delayed graft function. However, there was little difference between live donor kidneys and deceased donor kidneys that had not shown delayed graft function. Molecular changes did not predict future biopsies for clinical indications, rejection episodes, functional deterioration, or allograft loss. Despite the fact that cases with T cell mediated rejection (n=9) were treated and those with borderline (n=20) not, and both showed a similar molecular phenotype, no difference in terms of outcome between these two Banff groups were observed (figure 1b).

Figure 1

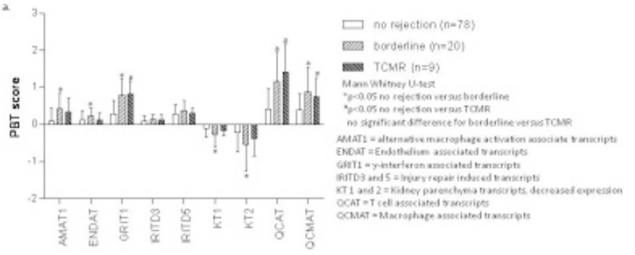

b.

	borderline	TCMR	p-value
ΔeGFR 6-weeks to two-years	1.15 ± 14.6	-0.67 ± 11.2	ns
ΔIFTA 6-weeks to 6-months	1.20 ± 1.2	1.22 ± 1.9	ns
%total cortical infiltrate (Banff ti-score) in 6-month sequential protocol biopsy	13.80 ± 18.1	14.00 ± 10.9	ns

Conclusions: Thus while detecting T cell-mediated inflammation, the molecular phenotype of early protocol biopsies mostly reflects the injury-repair response to implantation stresses, and has little relationship to future events and outcomes, independent of any therapeutic intervention.

1478 Fibrillary Glomerulonephritis: A Report of 66 Cases from a Single Institution.

S Nasr, A Valeri, L Cornell, M Fidler, S Sethi, N Leung, F Fervenza. Mayo Clinic, Rochester, MN; Columbia University, New York, NY.

Background: Fibrillary glomerulonephritis (FGN) is a rare primary glomerular disease. Most previously reported cases were idiopathic. In order to better define the clinical-pathologic spectrum and prognosis, we report the largest single-center series with the longest follow-up.

Design: The characteristics of 66 FGN patients who were seen at our institution between 1993-2010 are provided.

Results: The mean age at diagnosis was 53 yrs. Ninety-five percent of patients were Caucasian and the female:male ratio was 1.2:1. Underlying malignancy (most commonly carcinoma), dysproteinemia, or autoimmune disease (most commonly Crohn's disease, SLE, Graves' disease, and idiopathic thrombocytopenic purpura) were present in 23%, 17%, and 15% of patients, respectively. Presentation included proteinuria (100%), nephrotic syndrome (38%), renal insufficiency (66%), hematuria (52%), and hypertension (71%). The most common histologic pattern was mesangial proliferative/sclerosing GN (71%) followed by membranoproliferative GN (15%). Endocapillary proliferative GN, crescentic GN, membranous GN (MGN), and diffuse sclerosing GN were rare patterns, seen in 6%, 5%, 2%, and 2% of cases. By definition, the glomerular deposits were Congo-red negative. By immunofluoresence (IF), all 66 cases showed glomerular positivity for IgG and in 11% the deposits were monoclonal. Tubular basement membrane deposits on IF were seen in 14% of cases. On electron microscopy, the fibrillary deposits were seen in the mesangium in 98% of cases and in the GBMs in 85%. In the single case with MGN pattern on light microscopy, the fibrillary deposits were present in the subepithelial zone of the GBMs associated with spike formation, without mesangial deposits. In all 66 cases, the fibrils were randomly-oriented and straight, with a mean diameter of 18 nm (range of means, 9-26 nm). During an average of 52.3 mo of follow-up for 61 patients with available data, 13% had complete or partial remission, 43% had persistent renal dysfunction, and 44% progressed to ESRD. The disease recurred in 36% of 14 patients who received a kidney transplant. Independent predictors of ESRD by multivariate analysis were older age, higher creatinine and proteinuria at biopsy and higher percentage of global glomerulosclerosis.

Conclusions: Underlying malignancy, dysproteinemia, or autoimmune diseases are not uncommon in patients with FGN. Prognosis is poor, although remission may occur in a minority of patients without immunosuppressive therapy. Age, degree of renal impairment at diagnosis, and degree of glomerular scarring are predictors of renal survival.

1479 Hypertension-Associated Nephrosclerosis: Does the Activation of Parietal Epithelial Cells (PECs) Differ between African Americans and Caucasians?

MO Odubanjo, B Smeets, MJ Moeller, AB Fogo. Vanderbilt University Medical Center, Nashville, TN; University Hospital of RWTH, Aachen University, Germany.

Background: Loss of podocytes is critical for progressive glomerulosclerosis. Parietal epithelial cells (PECs) may act as stem cells that replenish podocytes. Our aim was to determine the extent to which PECs are activated following hypertension-associated injury in African Americans (AA) and Caucasians (C).

Design: Activated PECs were identified by CD44 staining. We scored activated PECs in anatomical parietal and podocyte locations in glomeruli without lesions and glomeruli with segmental sclerosis (SS) and/or adhesions, and the total number of activated PECs was quantified for globally sclerosed (GS) glomeruli.

Results: A total of 352 glomeruli from 31 biopsies were analyzed. 209 glomeruli showed no lesions (50 AA, 159 C), 110 (73 AA, 37 C) showed global sclerosis, 12 (9 AA, 3 C) showed SS and/or adhesions, 19 (10 AA, 9 C) showed periglomerular fibrosis, and 2 (both AA) showed extracapillary proliferation with no GBM breaks or

fibrinoid necrosis. The distribution of glomerular lesions differed between AA and C, with glomeruli without lesions being more commonly seen in C, and GS and SS being more common in AA.
Activated PECs were detected in 21 glomeruli, 14 AA and 7 C (8 glomeruli without lesions: 5 AA and 3 C; 4 with GS: 3 AA and 1 C; 4 with SS and or adhesions: all AA; 3 with periglomerular fibrosis: all C; and 2 with extracapillary proliferation: both AA).
There was an average of 7.2 CD44+ cells in parietal location/ glomerulus in AA versus 1.7/ glomerulus in C.
In 4 of the 12 glomeruli with SS and/or adhesions, CD44+ cells were most common in a parietal location and more commonly, away from the lesion than adjacent to the lesion (4 glomeruli, on average 7.25/glomerulus, 6 in parietal location (1 in the lesion and 5 in the non-lesion area) and 1.25 in podocyte location (P value < 0.001 for lesion versus non-lesion area).
Conclusions: Activated PECs were present more commonly in AA than C, even in glomeruli without sclerosing lesions. This supports the possibility that abnormalities in the differentiation and regulation of the glomerular epithelial cell population could contribute to the pathogenesis of the glomerular scarring in arterionephrosclerosis. Whether these activated PECs contribute to sclerosis or represent regenerative repair responses awaits further study.

1480 Significance of p53 Expression and Tubulo-Interstitial Inflammation in Renal Transplant with BK Virus Nephropathy.

R Ohashi, D Dadhania, M Suthanthiran, SV Seshan. Weill Cornell Medical Center, New York, NY; Nippon Medical School, Tokyo, Japan.

Background: P53 expression has been localized in BKV positive nuclei, but its significance remains obscure in BK virus nephropathy (BKVN). We assessed p53 expression in renal tubular nuclei in BKVN renal tranplant biopsies (TrBx) and its association with other histological parameters.
Design: Tubular expression of p53 and BK virus was immunohistochemically quantified in renal TrBx with BKVN (n=31) in serial sections. Morphological features including viral cytopathic changes (vcc), interstitial inflammation (i), tubulitis (t), interstitial fibrosis (ci) and tubular atrophy (ct) were scored as; 0-3. The frequency of interstitial inflammatory cell types (polymorphonuclear leukocytes PMN, plasma cells PC, and CD3+ and CD20+ lymphocytes) were scored as 0-3. 15 cases with an increase in creatinine of more than 0.5 mg/dl after BKVN diagnosis were classified as decline in function group (BKVN-DF) and the remaining 16 BKVN without an increase in creatinine were classified as stable function group (BKVN-SF). As control BKV – TrBx, acute tubular injury (ATI), acute cellular rejection (ACR), acute antibody mediated rejection and interstitial fibrosis and tubular atrophy, were used and stained for tubular p53.
Results: In BKVN, p53 co-localized with BKV within tubular nuclei showing intranuclear inclusions and hyperchromasia. P53 expression was higher in BKVN than BKV – control cases ($p<0.05$), the latter showing p53 in tubules with injury and regenerative changes (ATI) or tubulitis (ACR). In BKVN, although there was proportional correlation between the numbers of p53+ and BKV+ cells ($r=0.72$, $p<0.05$), the total p53+ cell number was higher than BKV+ cells in cases with moderate to severe inflammation (i2, i3, t2, t3)($P<0.05$). In cases with higher grades (2-3) of PMN, PC and CD3+ inflammatory infiltrates, the p53+ cells were also more than BKV+ cells ($p<0.01$). In BKVN-DF group, the total p53+ cell number was significantly higher than BKVN-SF (7.8±4.7/HPF vs 4.8±3.0, $p<0.05$) while BKV+ cells showed no significant difference ($p = 0.7$).
Conclusions: In BKVN, co-localization of p53 and BKV indicates a direct link between p53 and BKV infection within tubular nuclei. Increased p53+ cells in cases with significant inflammation may suggest augmented p53 expression by accompanying active interstitial inflammation. The increased ratio of tubular p53+ to BKV+ cells in BKVN may serve as a potential prognostic histologic marker.

1481 Microcirculation Endothelial Cell Proliferation Is Specifically Increased in Antibody-Mediated Rejection as Compared to Other Diseases in Kidney Transplants.

S Osasan, J Chang, Y Ozluk, DG de Freitas, M Mengel, P Halloran, B Sis. University of Alberta, Edmonton, Canada.

Background: Antibody-mediated rejection (ABMR) is mediated by antibodies against donor HLA, leading to allograft injury and failure. We hypothesized that there is greater endothelial repair response in ABMR compared to other diseases in kidney transplants.
Design: We related microcirculation endothelial cell cycling and density of peritubular capillaries(PTC) to lesions, diagnoses, and whole-genome microarrays in 100 non-selected kidney transplant biopsies for cause(BFC) and 20 normal kidney implantation biopsies from living donors. We performed double immunostaining and quantified the microcirculation endothelial cell cycling (Ki-67+CD31+ glomerular capillaries and PTCs) and the CD31+ PTC density by cell counting in the entire renal cortical biopsy area.
Results: The BFC showed higher numbers of cycling microcirculation endothelial cells in comparison to normal controls ($p=0.001$). The endothelial cell cycling was specifically increased in ABMR compared to other diseases i.e. T cell-mediated rejection, glomerulonephritis, and others.

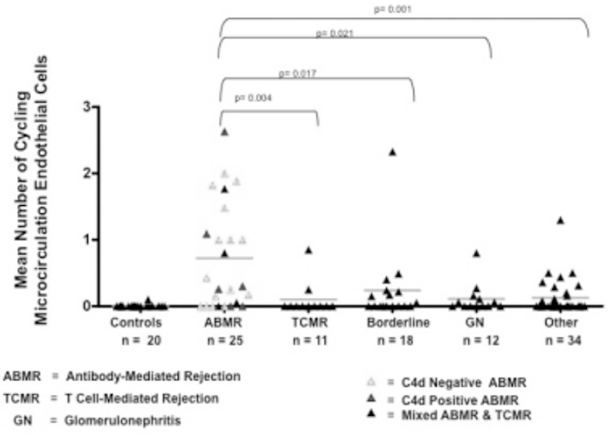

This increase correlates with microcirculation lesions (glomerulitis, peritubular capillaritis, transplant glomerulopathy), and C4d staining ($p<0.05$). Furthermore, It also correlates with transcript sets representing the molecular burden of active ABMR($p<0.05$). The PTC density was lower in biopsies for cause when compared to normal controls ($p<0.001$). However, the PTC density did not differ among diagnoses and was not correlated with time post-transplant, scarring or other lesions.

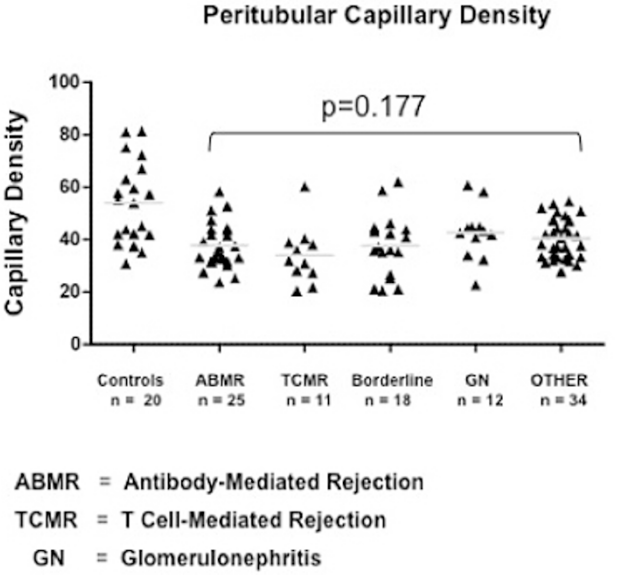

Conclusions: We conclude that endothelial repair response is specifically increased in kidneys with ABMR, reflecting the burden of microcirculation injury. In contrast to previous observations, there is no evidence for reduced PTC density in kidneys with scarring.

1482 Expansion of the Parietal Cell Compartment in Collapsing Glomerulopathy.

MF Palma Diaz, G Giannico, S Phillips, Y Shyr, AB Fogo, CE Alpers, VD D'Agati. Columbia University, New York, NY; University of Washington, Seattle; Vanderbilt University, Nashville, TN.

Background: Glomerular epithelial cell hyperplasia and pseudocrescent formation overlying collapsed segments are defining features of collapsing glomerulopathy. The proliferative potential and relative contributions of dedifferentiated podocytes (PODs) versus parietal epithelial cells (PECs) to the glomerular epithelial hyperplasia remain controversial.
Design: We examined 44 biopsies of primary collapsing focal segmental glomerulosclerosis classified by the Columbia classification. Serial paraffin sections were stained with antisera to claudin (an occludens junction protein expressed on PECs and tubular cells), WT-1 (a zinc finger transcription factor expressed by mature PODs) and Ki-67 (proliferation marker). Every glomerulus (including collapsing, NOS and histologically normal phenotypes) in each biopsy was scored for positive cells in lesional vs non-lesional segments and dichotomized for visceral and parietal anatomic locations. Co-localization was investigated by superimposition of serial images.
Results: Histologically normal glomeruli displayed restriction of claudin to PECs lining Bowman's capsule, whereas WT-1 was expressed by visceral PODs and rare parietal PODs, suggesting non-overlapping lineage-specific markers. Variable numbers of claudin+, Ki67+ cells could be identified lining Bowman's capsule in collapsing, NOS and histologically normal glomeruli. There was widespread downregulation or complete loss of WT-1 overlying collapsed segments with swollen PODs. Only rare PODs bearing WT-1 were also Ki-67+. By contrast, most Ki-67+ glomerular epithelial cells

were strongly claudin+, indicating predominant expansion of the parietal compartment. Claudin+ cells typically extended out from Bowman's capsule to bridge and overlie the glomerular tuft in acute collapse and more chronic NOS lesions, often mimicking PODs, and formed the majority of cells in the pseudocrescents.

Conclusions: Loss of WT-1 from PODs in collapsing glomerulopathy supports the concept of the dysregulated podocyte phenotype in the pathogenesis of this lesion. PECs can populate the collapsed tuft and comprise the majority of cell cycle-engaged cells in primary collapsing glomerulopathy.

1483 Evaluation of Nonneoplastic Renal Parenchyma in Partial Nephrectomies.

C Parra-Herran, M Garcia-Roig, M Jorda, M Gorin, B Kava, M Manoharan, M Soloway, G Ciancio, M Garcia-Buitrago. U Miami Jackson Memorial Hosp, FL.

Background: Pathologic changes in nonneoplastic renal parenchyma (NNRP) are associated with progression to renal failure. Compared to total nephrectomies, evaluation of those changes in partial nephrectomies (PN) is less consistent. We postulate that pathologic changes in the NNRP of PN can be adequately assessed and may have therapeutic impact after surgery.

Design: We retrieved histologic material of patients who underwent PN in a 12-year-period. Demographic data, comorbilities, tumor features, creatinine levels and glomerular filtration rate (GFR) pre and post surgery was collected. NNRP was assessed for glomerular, tubulointerstitial and vascular changes. Peritumoral parenchyma (1mm) was not evaluated. The findings were correlated with clinical data.

Results: A total of 174 patients underwent PN. Of those, 104 were available. Ten patients were excluded due to lack of NNRP. 94 patients (57M, 37F) were studied. The patient's mean age was 58.5 years. Patient's comorbilities included Diabetes mellitus (DM, 18%), hypertension (HTN, 53%), and coronary artery disease (CAD, 12%). Resected tumors were neoplastic (conventional renal cell carcinoma 64%, papillary 17%, others 17%) and nonneoplastic (2%). The most frequent NNRP lesions included mesangial expansion (24%), atherosclerosis (22%), interstitial fibrosis (18%), arteriolosclerosis (7%) and >20% global glomerulosclerosis (6%). Presence of these combined pathologic changes was associated with HTN, DM and CAD (Table 1).

CORRELATION BETWEEN PATHOLOGIC CHANGES, COMORBILITIES AND RENAL FUNCTION (RF)

		PATHOLOGIC CHANGES		
		PRESENT	ABSENT	TOTAL
HTN	YES	49	1	50
	NO	39	5	44
	TOTAL	88	6	94
DM	YES	16	1	17
	NO	71	6	77
	TOTAL	87	7	94
CAD	YES	11	0	11
	NO	74	9	83
	TOTAL	85	9	94
DECREASED RF	YES	21	1	22
	NO	51	3	54
	TOTAL	72	4	76

Renal function data was available in 76 patients. Significant change (>20% raised creatinine and decreased GFR) between pre and postoperative period was seen in 22 patients, 21 showed NNRP changes. Of 39 patients with no history of comorbilities, vascular (82%) and tubulointerstitial changes (33%) were seen. None of these patients showed glomerular changes.

Conclusions: Optimal evaluation of NNRP can be achieved in the vast majority of PN (90% in our series). Pathologic changes are found in a significant amount of cases, including those without history of comorbilities, and may be associated with risk of RF impairment. Thus, adequate pathologic assessment of NNRP should always be performed in PN, since it can alert the clinician about progression of renal disease and need for close follow up.

1484 Significance of IgG4 Immunostaining in Plasma Cell-Rich Tubulointerstitial Nephritis (TIN).

Y Raissian, SH Nasr, CP Larsen, ME Fidler, S Sethi, A Bhalodia, LD Cornell. Mayo Clinic, Rochester, MN; Nephropath, Little Rock, AR; Univ of Louisiana, Shreveport.

Background: A number of conditions may cause TIN. IgG4 staining has been proposed as a tool to identify TIN as part of IgG4-related systemic disease(IgG4-RSD), but the sensitivity and specificity of IgG4 staining has not been established.

Design: A database search was performed for all cases within one year(2007) with a final diagnosis of TIN, including cases with glomerular disease; causes of TIN were based on clinical and laboratory data. Light microscopy slides of TIN cases were reviewed for increased plasma cells, defined as >5 cells/40x field in ≥3 fields. Cases with increased plasma cells were stained for IgG4 by immunohistochemistry. For comparison, IgG4 staining was also done on TIN cases in patients with clinical features suspicious for IgG4-RSD(n=23), TIN in patients with a history of pancreatitis(n=17), pauci-immune crescentic glomerulonephritis(GN)(n=14), Sjogren TIN(n=14), drug-related(n=5), chronic pyelonephritis(n=2), and unknown or autoimmune cases(n=4). IgG4 stains were graded in the most concentrated area per 40x field as: no increase <5 cells, mild 5-10, moderate 11-30 and marked >30.

Results: Within the given year, 414 cases of TIN were found including 167 cases with associated non-diabetic glomerular disease. Of these, 83/414(20%) had at least moderate increase in plasma cells, with etiology as follows: 25% drug effect, 21% unknown, 20% associated with pauci-immune GN, 14% with other glomerular disease(immune-mediated crescentic GN,FSGS,diabetes), 10% autoimmune disease, 2% pyelonephritis, 2% IgG4-RSD, 1% oxalate nephropathy. 15/83(18%) showed moderate or marked increase in IgG4+ plasma cells; these cases were pauci-immune GN(n=7), TIN due to drug(n=3), other glomerular disease(n=2), pyelonephritis(n=1), and IgG4-RSD(n=1). In the comparison groups, 23/23(100%) of the IgG4-RSD showed moderate to marked increase in IgG4+ cells, 6/24(25%) cases of pauci-immune GN, 1/14(7%) Sjogren TIN, and 0/17(0%) TIN in patients with a history of pancreatitis, 1/2(50%) with pyelonephritis, and 0/4(0%) TIN of unknown etiology showed increased IgG4+ cells.

In total, excluding IgG4-RSD and pauci-immune GN, 9/107(8%) of TIN studied showed at least moderate increase in IgG4+ plasma cells. If pauci-immune GN is excluded, the IgG4 stain has a sensitivity of 100% and a specificity of 92% for TIN as part of IgG4-RSD.

Conclusions: IgG4 is a sensitive and specific marker for diagnosis of TIN as part of IgG4-RSD. Increased IgG4+ cells may also be seen in pauci-immune crescentic GN; rare other TIN cases may show increased IgG4+ cells.

1485 Membranous Glomerulonephritis with Crescents.

EF Rodriguez, SH Nasr, S Sethi, ME Fidler, LD Cornell. Mayo Clinic, Rochester, MN.

Background: Only rare cases of membranous glomerulonephritis (MGN) with crescents have been reported. We present a series of ANCA-negative MGN with crescents.

Design: We searched the pathology database at our institution from 1/1994-9/2010 for cases of MGN with crescents from non-lupus patients who had negative ANCA and anti-GBM antibodies. We examined in detail the clinicopathologic features and outcomes in these patients.

Results: A total of 4215 cases of MGN, both primary and secondary, were identified. Of these, 12 patients (0.3%) had ANCA- and anti-GBM-negative crescentic MGN. The mean age at diagnosis was 47 yrs (range 5-86); half were female. At presentation, all patients had proteinuria (mean 11.3 g/d; range 3.3-26) and hematuria, and 10/12 (83%) patients had renal failure (mean serum Cr 3.3 mg/dL; range 0.4-10). ANA was negative in 9 patients and transiently or weakly positive in 3 patients; no patients had hepatitis B or C infection. On light microscopy, glomeruli showed on average 26% involvement by crescents (range 5-73%), with 10/12 cases showing <50% crescents. All cases showed a membranous pattern; 6 cases showed mild mesangial and 2 showed segmental endocapillary proliferation. By immunofluorescence, all cases with glomeruli (n=11) showed a membranous pattern with staining for IgG, kappa, and lambda, and all but one showed C3; 2 cases showed staining for C1q (trace and 2+) and one showed trace IgA. By electron microscopy, most cases showed stage II MGN. 2 showed mesangial deposits, and one showed subendothelial deposits. Endothelial tubuloreticular inclusions were seen in one case. Follow-up clinical data were available in all 12 cases (mean 32 mos; range 0.5-138). 10 patients were treated, 5 with high-dose prednisone and cyclophosphamide, 2 with steroids and a calcineurin inhibitor (tacrolimus or cyclosporine), 2 with prednisone alone, and one with enalapril alone. 2 patients progressed to ESRD, at 0-2 mos post-biopsy. The mean serum Cr of the other 10 patients at follow-up was 1.6 mg/dL (range 0.5-4.1), with 8/10 (80%) patients showing elevated serum Cr. 6 of 7 patients with available data and without ESRD had ≥1 g/d proteinuria at follow-up. One patient later had an equivocal MPO titer, and another had a positive MPO titer 8 mos after biopsy. No patients developed lupus. 2 patients had follow-up biopsies, at 1.3 and 4.6 years later: one had MGN without crescents, and the other had MGN with focal crescents.

Conclusions: Crescentic MGN is a rare variant of MGN that usually presents with heavy proteinuria, hematuria, and renal failure. The prognosis is variable and the disease may respond to therapy, but most patients develop chronic renal failure.

1486 Telemicroscopy for the Evaluation of Donor Kidney Biopsies.

E Sadimin, W Chen, A Osband, W Reitsma, D Laskow, J Joseph, B Fyfe. UMDNJ – Robert Wood Johnson Medical School, New Brunswick, NJ; New Jersey Sharing Network, New Providence.

Background: Pathologists play a vital role in the evaluation of kidney donor biopsies, largely related to accurate measurement of % global glomerulosclerosis (%GG). We have previously shown lack of correlation for %GG using light microscopy (LM) with manual slide manipulation. This study examines the correlation of %GG measurements using telemicroscopy (TM) enhanced with Computer Assisted Microscopy (CAM) software.

Design: Thirty-seven kidney donor biopsies with prior LM analysis performed at regional transplant centers and at our institution were studied with TM. The real time robotic TM incorporates an Olympus BX51 microscope with a robotic stage controlled by CAM software. The software provides the user an overview of the specimen that is used to select the region of interest (ROI). The ROI is overlaid with a grid map. Each grid cell corresponds to one non-overlapping screen of view. The user sets the desired objective and activates the program to advance from grid cell to grid cell. Analyzed cells are highlighted by a color change. The specimens were evaluated for %GG and total number of glomeruli using a 10x grid with full support for panning, zooming and focusing. The correlation coefficient is calculated using MedCalc.

Results: The correlation coefficient for %GG and total glomeruli measured by TM is significantly higher than LM.

	LM1	LM2	TM1	TM2
LM1	NA	0.6093	0.5504	0.5319
LM2	0.7421	NA	0.8744	0.8645
TM1	0.7707	0.8990	NA	0.9959
TM2	0.7582	0.8887	0.9944	NA

Table 1. Correlation coefficients between different measurements for total glomeruli (bottom left half) and %GG (top right half).

In most cases the numbers obtained by TM are higher than the numbers obtained by LM.

Conclusions: TM supported by sophisticated software (CAM) is a more accurate and reproducible technique than LM for assessing %GG in donor kidney biopsies. CAM software prevented review of overlapping fields, highlighted areas already viewed and

was essential to the ease of use and reproducibility. TM also forms a foundation for more descriptive quantitative studies of donor kidney biopsies (e.g. density distribution of globally sclerosed glomeruli) potentially ultimately leading to increased utilization of this precious resource.

1487 Acquired Glomerular Lesions in Patients with Down Syndrome.

S Said, L Cornell, S Sethi, M Fidler, O Al Masri, J Marple, S Nasr. Mayo Clinic, Rochester; Sheikh Khalifa Medical City, Abu Dhabi, United Arab Emirates; Lincoln Nephrology & Hypertension, Lincoln.

Background: The long-term survival of persons with Down syndrome has dramatically increased over the past 50 years, largely due to improvement in medical care. Renal disease is thought to be infrequent in these patients (pts) and data regarding renal biopsy are very limited. The aim of this study was to examine the clinicopathologic spectrum of pts with Down syndrome who underwent renal biopsy.

Design: We reviewed the characteristics of 16 pts with Down syndrome who underwent native renal biopsies that were processed at our laboratory from 1997 to 2010.

Results: The mean age at biopsy was 28 yrs (range 13-45). Eleven pts were Caucasian and 5 were African Americans. The male:female ratio was 1.6:1. History of hypothyroidism was present in 6 pts, congenital heart disease in 2, and congential urologic abnormalities in 1. Clinical presentations included renal insufficiency (15 pts, mean S. creatinine 3.4 mg/dl (range 0.7-15)), proteinuria (all pts, including 2 with nephrotic syndrome, mean 24h urine protein 3.6 g (range 0.4-24)), and hematuria (14 pts, including 3 with gross hematuria). The glomerular diseases found on biopsy were IgA nephropathy (IgAN)(n=5 pts), focal segmental glomerulosclerosis (FSGS) (n=3), membranoproliferative GN (MPGN) (n=2), acute post-infectious GN (APIGN) (n=2), ANCA-associated pauci-immune crescentic GN (PICGN)(n=2), membranous GN (n=1) and lupus nephritis (LN) class III (n=1). Mild dilatation of the urinary space was seen in 7 pts. Follow up (mean 47 mos, range 2-141) was available on 15 pts (94%). Two pts had complete remission; 1 of whom had nephrotic syndrome due to membranous GN that was treated with immunosuppressive agents (IS) (steroids and cyclophosphamide) and the other one had nephritic syndrome due to APIGN that was treated with IS (steroids). Eight pts (4 with IgAN, 2 with FSGS, 1 with LN III, and 1 with APIGN) had persistent renal dysfunction. Three of these pts (1 with IgAN, 1 with FSGS, and 1 with LN III) were treated with IS. The remaining 5 pts (2 with PICGN, 2 with MPGN, and 1 with FSGS) progressed to ESRD, 2 of whom died. Three of these 5 pts (2 with PICGN and 1 with MPGN) were treated with IS. One pt with MPGN received a succesful kidney transplant without histologic evidence of recurrence.

Conclusions: With prolonged survival, a growing number of pts with Down syndrome is expected to develop renal disease. A wide spectrum of acquired glomerular diseases can be seen in these pts. Renal biopsy is necessary to determine the type of glomerular lesion, appropriate treatment, and prognosis.

1488 Arteriolar Sclerosis in Tumor Nephrectomy Specimens Is Prognostically Significant.

SP Salvatore, SN Reddy, EK Cha, JS Rosoff, SV Seshan. Weill Cornell Medical College, New York.

Background: Recent studies have shown that evaluating non-tumor portions of tumor nephrectomy specimens is useful in diagnosing non-neoplastic renal disease. The purpose of this study is to determine the frequency of medical renal disease and to assess the prognostic significance of the degree of vascular sclerosis in the long term follow-up of tumor nephrectomy patients.

Design: We reviewed non-neoplastic kidney H&E stained slides of 232 cases from 1998 to 2005. Sixteen cases were excluded from the study (6 tumor compression, 5 no uninvolved kidney, 5 embolization/ infarction). PAS staining, immunofluorescence, and/ or electron microscopy was performed where appropriate. Vascular sclerosis was scored from 0-3, mild, moderate and severe. Follow-up of at least 1 year was evaluated in 101 cases. The degree of vascular sclerosis was compared to the change in the creatinine level, pre-surgery to follow-up (Table 1).

Results: Of the 216 cases reviewed, 47 had new pathologic diagnoses (21%): diabetic nephropathy 21, hypertensive nephropathy 11, focal segmental glomerulosclerosis 6, collapsing glomerulopathy 2, acute pyelonephritis, thrombotic microangiopathy, atheroembolic disease, granulomatous interstitial nephritis, reflux nephropathy, proliferative glomerulonephritis, and membranous glomerulonephritis 1 each. Eighty percent (80%) of the cases with additional non-neoplastic diagnoses and follow-up showed severe arteriolar sclerosis. Global glomerulosclerosis (GS) was higher in cases with more severe vascular sclerosis, mean 4.5% GS (mild) versus 17% GS (severe). Three patients, all diabetic nephropathy, progressed to end stage renal disease from 1 to 4 years after nephrectomy.

Arterioles	N	mean Cr difference (mg/dL)	p value	mean f/u (yrs)
mild	42	0.3	0.006*	5.6
moderate	33	0.4	0.02*	5.1
severe	26	0.8	n/a	4.9
Arteries				
mild	47	0.3	0.09	5.9
moderate	33	0.5	0.23	4.2
severe	21	0.7	n/a	4.4

*statistically significant

Conclusions: Non-neoplastic renal pathology can be evaluated in the majority of tumor nephrectomy specimens with 21% having additional diagnoses. The degree of arteriolar sclerosis but not arteriosclerosis is predictive of significantly higher creatinine levels and subsequent decline in renal function at follow-up in post-nephrectomy patients. The prognostic implications of the non-tumor pathology are therefore important in patients with reduced renal mass.

1489 Membranoproliferative Glomerulonephritis Secondary to Dysfunction of the Alternative Pathway of Complement.

S Sethi, F Fervenza, Y Zhang, S Nasr, J Vrana, RJH Smith. Mayo Clinic, Rochester, MN; Carver College of Medicine, Iowa City, IA; Mayo Clinic, Rochester.

Background: Dense Deposit Disease (DDD) is the prototypical membranoproliferative glomerulonpehritis (MPGN) in which dysregulation of the alternative pathway (AP) of complement results in accumulation of complement debris in glomeruli. MPGN with C3 deposition (GN-C3) is a recently recognized entity that bears many similarities to DDD. The aim of this study was to evaluate AP in cases of MPGN with C3 deposition.

Design: Five cases of MPGN with extensive C3 deposition were studied. IF was negative for immunoglobulins, C1q, kappa and lambda light chains, but showed extensive C3 deposition in the mesangium and along the GBM. EM showed electron dense deposits in the mesangium and along GBM (Case 1-3) but lacked the classic sausage shaped dense deposits of DDD, and were diagnosed as GN-C3. EM in case 5 exhibited the classic findings of DDD. Case 4 showed features of both DDD and GN-C3, with some loops showing electron dense deposits, and other loops showing sausage shaped deposits of DDD.

Results: Evidence of AP activation was demonstrable in all cases and included increased levels of soluble membrane attack complex (sMAC, all cases), positive AP functional assays (four cases), and a positive hemolytic assay (one case). Autoantibodies were found to C3 convertase (two cases) and to factor H (one case). Factor H mutation screening identified the H402 allele (all cases) and a missence factor H mutation (one case).

AP and genetic evaluation

	Case 1	Case 2	Case 3	Case 4	Case 5
CFH	1 copy H402	1 copy H402	2 copies of H402	2 copies of H402; c.2867 C>T p. Thr956Met	1 copy H402
CFI	No mutation	No mutation	No mutation	No mutation	No mutation
MCP	No mutation	No mutation	No mutation	No mutation	No mutation
CFB	ND	No mutation	No mutation	ND	No mutation
CFHR5	ND	No mutation	No mutation	ND	No mutation
AP functional assay	6.6% very low	109.0% normal	1.0% very low	5.5% very low	1.0% very low
Hemolytic Assay	Normal	1+	Normal	Normal	Normal
FH antibody	1:200	Negative	Negative	Negative	Negative
C3NeF	Negative	1:200	Negative	Negative	1:800
sMAC (Normal <0.30 mg/dL	0.46	0.41	1.23	0.93	0.31

Laser microdissection and mass spectrometry of glomeruli of GN-C3 showed a proteomic profile very similar to DDD.

Conclusions: Dysregulation of AP results in a spectrum of renal diseases that includes GN-C3 and DDD.

1490 De Novo AL Amyloidosis in Kidney Allograft.

S Sethi, S Nasr, M Fidler, L Cornell, Q Qian. Mayo Clinic, Rochester.

Background: Delayed onset of proteinuria in a renal allograft kidney can result from the development of transplant glomerulopathy, recurrent glomerular disease, diabetic nephropathy, etc. In this study, we describe a novel cause of proteinuria in the renal allograft

Design: We reviewed the clinicopathologic features of 4 kidney transplant patients (pts) who developed proteinuria late in the course. Renal allograft biopsy in all 4 pts showed de novo AL amyloidosis.

Results: Four pts who received a renal allograft 16, 18, 28 and 31 yrs ago developed proteinuria and progressive kidney dysfunction. Renal allograft biopsy showed AL amyloidosis in all renal compartments. Serum immunofixation performed after the kidney biopsy revealed monoclonal lambda light chains in all 4 pts. Bone marrow biopsy showed >10% plasma cells in 1 pt, 5-10% plasma cells in 2 pts, and <5% plasma cells in 1 pt. On follow up, 2 pts developed allograft failure. One of these two underwent autologous stem cell transplant which resulted in a complete hematological response. However, the remission did not prevent renal allograft failure. This pt received a second kidney transplant, which shows no evidence of allograft amyloidosis 1 yr post transplant. Of the remaining 2 pts, one suffered a sudden death during preparation for stem cell harvest and the other one was treated with prednisone and bortezomib which appears to have stabilized kidney function.

	Case 1	Case 2	Case 3	Case 4
Age/sex	59/M	60/M	45/F	62/M
Yrs between transplant and proteinuria	16	28	18	31
Native kidney disease	IgA nephropathy	GN 1	Bx of medulla, no amyloid	Congenital hypoplastic kidney
Immunosuppression	Cyclosporin/ prednisone	Azathioprine/ prednisone	Cyclosporin/ prednisone	Azathioprine/ prednisone
Symptoms*	Edema, foamy urine	Edema, foamy urine	UTI, 20 LB wt loss	None
S. creatinine* (baseline Cr)	4.4 (1.6 to 2.0)	1.4 (1.4)	1.8 (0.7-1.0)	1.3 (1.3-1.5)
U. protein *, g/24hr	10	8	2.5	1.4
S. albumin*, g/dL	2.0	2.0	2.9	3.9
Immunofixation	Lambda	Lambda	Lambda	Lambda
Bone marrow*	<5% plasma cells, no clonality	10% lambda light chain restricted plasma cells	5% lambda light chain restricted plasma cells	5-10% lambda light chain restricted plasma cells
Amyloid treatment	Prednisone/ Melphalan	Prednisone/ Bortezomib	Autologous stem cell transplantation	Prednisone/ Melphalan

* at the time of amyloid diagnosis, 1 Bx not done, presumed IgA

Conclusions: De novo AL amyloidosis should be considered in the differential diagnosis of late onset proteinuria in the renal allograft.

1491 Routine In-Situ Hybridization of Kidney Transplant Biopsies for BK Virus (BKV): Is It Justifiable?

C Singh, A Meares, JC Manivel, J Jessurun, SE Pambuccian, B Najafian. University of Minnesota, Minneapolis.

Background: BKV nephropathy (BKN) is an important cause of renal transplant dysfunction. BKN diagnosis requires observation of characteristic BK nuclear inclusions in tubular or parietal epithelial cells, and confirmatory nuclear staining by BK in-situ hybridization (BKISH) or SV-40 antibody. The triggers for performing BKISH or SV-40, besides suspicious cytopathic changes on biopsy, are +BK blood PCR or prior BKN history. In the absence of evident BK nuclear includions or relevant history, BKN may be missed by pathologists. However, the value of performing BKISH or SV-40 routinely on all renal transplant biopsies (Tx Bx) is not clear. Here we present the data from BKISH performed on renal Tx Bx routinely for one year at our institution.

Design: BKISH was performed on consecutive allograft biopsies over one year. Pathologists, who were not blinded to BKN previous history, were asked to predict presence of BKN on routine light microscopy slides before BKISH results were available. Predictions were compared to BKISH, as the gold standard.

Results: Of the 291 (M/F=166/125) Bx (age 45 ± 16 years) studied, 17 (6%) Bx had + BKISH, the majority of which (82%) were from male patients. Overall, pathologists' prediction was in agreement with BKISH in 91% of biopsies, while %agreement for +BKISH (pathologist call sensitivity) was 59% (Table 1) and for -BKISH (pathologist call specificity) was 93%. The pathologists' positive predictive value for BKN was 36%, while the negative predictive value was 97%. BKN was missed in 41% of +BKISH.

	BKISH+	BKISH-	
Positive Prediction	10	18	PPV*= 36%
Negative Prediction	7	256	NPV**= 97%
	Sensitivity= 59%	Specificity= 93%	

PPV*= Positive Predictive Value; NPV**= Negative Predictive Value

None of these missed cases had BKN prior history. While BKN overcalling rates were different among the pathologists (p=0.01), the undercalling rates were not statistically different. BKN overcalling was statistically significantly (P=0.04) and BKN undercalling was marginally (p=0.05) associated with presence of acute cellular rejection (ACR).

Conclusions: Most discrepancies between pathologists' call and BKISH resulted from overcalling BKN, mostly in Bx with ACR. Such discrepancies could have been resolved if BKN suspicion triggered a BKISH. Although only 6% of Bx had BKN, a substantial proportion (~40%) of BKN+ cases could have been missed by pathologists without performing BKISH. These studies suggest that BKN characteristic morphologic features are not sensitive enough to capture majority of positive cases, particularly in the presence of ACR.

1492 Urinary Polyomavirus Haufen Shedding Accurately Reflects Intrarenal Burden of Polyomavirus Nephropathy (PVN): Comparative Quantitative Analyses of Different Screening Techniques.

H Singh, K Tomasz, T Karen, V Derebail, D Randy, A Gasim, V Nickeleit. The University of North Carolina, Chapel Hill.

Background: We previously defined a new, qualitative noninvasive test to accurately diagnose PVN, a common infectious complication in renal allografts. The test is based on the detection of three dimensional cast-like polyomavirus (PV) aggregates, "Haufen", in voided urine samples. Urinary Haufen-testing is highly accurate for PVN (positive and negative predictive values > 95%).

Aim: Quantitative assessment of urinary Haufen shedding, viremia and viruria (by PCR, urine cytology) was performed and correlated with intrarenal signs of PV replication/ PVN (viral detection by immunohistochemistry: SV40-T antigen). **Hypothesis**: In comparison to conventional screening techniques, the degree of urinary Haufen shedding most accurately reflects the extent of intrarenal PV replication and "viral burden".

Design: Quantitative analysis of urinary Haufen shedding (number Haufen/mL), PCR assays (serum, urine), and quantitation of urinary decoy cell shedding (number decoy cells/ThinPrep® slide) were performed on 39 samples from 37 patients with concurrent biopsy proven PVN. Results were correlated with biopsy findings (PVN disease stage and number of cells / %tubules expressing SV40-T antigen). Statistics were performed using Kruskal Wallis testing with ties.

Results: Degree of intrarenal polyomavirus replication: The number of urinary Haufen/ mL showed the tightest correlation with the number of SV40-T expressing cells (correlation coefficient (cc) 0.86) and with the percentage of affected tubules (cc 0.70) in allografts with PVN (in comparison: cc viremia by PCR: 0.45; cc viruria by PCR: 0.45; cc decoy cells: 0.01). PVN disease stages: Only the number of urinary Haufen/mL showed a significant correlation with PVN disease stages ($p<0.0001$). Neither the degree of viremia nor viruria and decoy cell shedding correlated with PVN disease stages.

Conclusions: Haufen-testing is the most accurate noninvasive technique to diagnose PVN, predict PVN disease stages, and also to monitor the degree of polyomavirus replication. It may help to better assess the effectiveness of anti-viral therapy during persistent disease.

1493 Developing a Molecular Diagnosis of Antibody Mediated Rejection: Can Molecular Assessments Replace C4d?

B Sis, L Hidalgo, G Einecke, M Mengel, J Reeve, K Famulski, A Matas, B Kasiske, B Kaplan, P Halloran. University of Alberta, Edmonton, Canada; University of Minnesota, Minneapolis; University of Arizona, Tucson.

Background: When microcirculation lesions and HLA-antibody were used to define antibody-mediated rejection (ABMR), 63% of late kidney failures were attributable to ABMR, but many were C4d negative, suggesting that detection of this phenotype requires new diagnostic criteria (AJT 2009;9:2520-31). We previously showed that high endothelial gene set expression in kidney transplant biopsies with donor specific antibody (DSA) indicates active ABMR and predicts poor graft survival (AJT 2009;9:2312-23).

We hypothesized that measurement of individual endothelial transcripts in biopsies is a sensitive and specific method to diagnose ABMR.

Design: We studied 403 kidney transplant biopsies for cause from 315 patients by histopathology, C4d staining (368/403), antibody testing (355/403), and microarrays. ABMR was defined by histology/serology: microcirculation lesions (g>0 and/or ptc>0 and/or cg>0) plus DSA: Of 403 biopsies, 24 had C4d+ ABMR, 45 C4d negative ABMR, and 14 mixed rejection. The new molecular/serology definition of ABMR included high endothelial gene expression in the presence of DSA.

Results: We evaluated expression of three endothelial transcripts: SOX7 (SRY-box 7), CDH5 (cadherin 5), and VWF (von Willebrand factor). In a training set (n=201), we selected a cut-off signal for each gene for detecting ABMR (histology/serology) with at least 80% sensitivity by ROC curve analysis.

Applying the same cut-offs in an independent set (n=202), SOX7 plus DSA showed 88% sensitivity and 90% specificity, and combined SOX2/CDH5/VWF plus DSA showed 90% sensitivity and 86% specificity for ABMR, whereas, C4d showed 49% sensitivity and 96% specificity.

A. ROC analysis of endothelial transcripts in two independent sets of biopsies for cause to detect ABMR defined by histology/serology

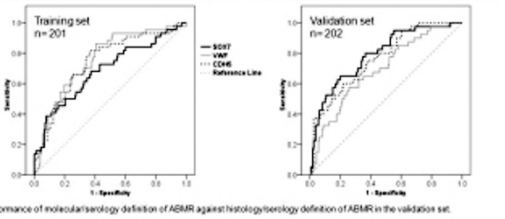

B. Performance of molecular/serology definition of ABMR against histology/serology definition of ABMR in the validation set.

		ABMR 0	ABMR 1	sensitivity	specificity	accuracy
SOX7 or CDH5 or VWF + DSA present	1	22	36	0.90	0.86	0.87
	0	136	4			
SOX7 + DSA present	1	16	35	0.88	0.90	0.89
	0	142	5			
VWF + DSA present	1	13	25	0.63	0.92	0.86
	0	145	15			
CDH5 + DSA present	1	13	27	0.66	0.92	0.87
	0	145	13			
C4d	1	6	19	0.49	0.96	0.86
	0	139	20			

Conclusions: Thus measuring a few endothelial transcripts in biopsies from kidneys with alloantibody is a highly sensitive and specific method to detect ABMR, and is more sensitive than C4d. Endothelial molecular parameters should be incorporated into the Banff classification to improve diagnosis of ABMR.

1494 Microcirculation Inflammation in Kidney Transplant Biopsies: Relationship to Diseases and Transplant Outcomes.

B Sis, G Jhangri, J Riopel, H Mahsin, J Chang, M Mengel, D de Freitas, J Sellares, S Osasan, B Kaplan, P Halloran. University of Alberta, Edmonton, Canada; University of Arizona, Tucson.

Background: We studied the significance of microcirculation inflammation – glomerulitis and peritubular capillaritis – in kidney transplants in relationship to diseases and outcomes.

Design: We examined 221 renal allograft biopsies for cause from 169 patients (median follow-up after biopsy 32 months).

Results: Glomerulitis (g) and peritubular capillaritis (ptc) were associated with antibody-mediated rejection (ABMR) (63% and 70%, respectively), but were not specific because they were also seen in other diseases (T cell-mediated rejection, glomerulonephritis, acute tubular necrosis). In univariate analysis, all g>0 grades and ptc2,3 predicted poor survival, but ptc1 did not. In multivariate analysis, the combination of g>0 plus ptc>1 independently predicted poor survival, but either g>0 or ptc>1, C4d, alloantibody, and transplant glomerulopathy did not. Transplant glomerulopathy with g>0 plus ptc>1 showed accelerated graft loss, but transplant glomerulopathy without this combination showed an indolent course. The majority (89%) of biopsies with g>0 plus ptc>1 was antibody-mediated rejection (C4d +/-). In multivariate analysis of ABMR patients, concurrent g>0 plus ptc>1 was the only independent predictor of graft loss.

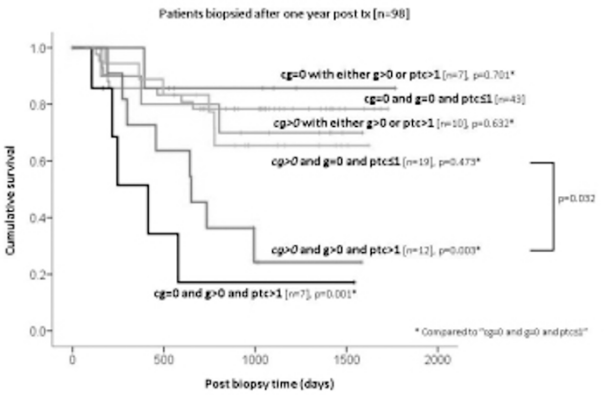

Conclusions: Thus, the combination of glomerulitis (g>0) plus peritubular capillaritis (ptc>1) in the presence of DSA should be recognized as active antibody-mediated rejection with a high risk for graft failure, without requiring C4d staining.

1495 Segmental Collapsing Capillary Tufts (SCCT) in Diabetic Glomeruli.

LC Stout. University of Texas Medical Branch, Galveston.

Background: Capillary obliteration is obvious in large Kimmelstiel-Wilson nodules, but its mechanism is unknown in the far more prevalent diffuse lesion, where expanding mesangium just seems to fill the glomerulus until it becomes obsolescent. This report describes novel segmental collapsing capillary tufts (SCCT) in 2 of 25 diabetics, 1 with Type 1 (T1DM) and 1 with Type 2 (T2DM) diabetes.

Design: SCCT were found by chance in a study of glomerular changes in 74 diabetics (end stage renal disease excluded) and 59 matched controls from consecutive autopsies at our hospital. The present study group consisted of 25 of the diabetics that had any degree of diabetic glomerulopathy and 12 matched controls. All 37 cases had 18 variously stained paraffin embedded 4 µm serial sections. One hundred glomeruli from each case were reviewed in section 9 (PAS). Nine to 15 glomeruli were completely traced in each of 2 diabetics and 2 controls that had PolyBed 812 embedded toluidine blue stained 1µm serial sections.

Results: SCCT were first seen in 1 µm serial sections in the T1DM case that had 16 SCCT in 8 of 9 complete and 4 partial glomeruli (5 gomeruli had 1, 1 had 2, 1 had 3 and 1 had 6 SCCT). Six SCCT in 5 glomeruli were large. No definite SCCT were found in the 4 µm sections from the same case. SCCT were called early [mild decrease in capillary lumen size and glomerular capillary basement membrane (GBM) width], mid (moderately decreased lumen size and GBM width), and late (collapsed autolyzed masses of barely recognizable capillaries and mesangium). SCCT were called small (in-situ capillary segments) or large (detached capillaries and mesangium up to 35 x 60 x >55µm in size. Three large SCCT were attached to the tuft by a single capillary, the GBMs of which were contiguous but abruptly thinned in the SCCT. Mesangium occupied the intracapillary space in the tuft at the junction. One T2DM case had 1 probable and 1 possible large SCCT in paraffin sections.

Conclusions: The decreased intraluminal volume and thin GBMs of SCCT suggested decreased perfusion. This and their seemingly autolytic demise suggested a gradual rather than a sudden decrease in flow, possibly due to diabetic mesangial expansion and/or disordered mesangial contraction. Inter or intralobular small anastomotic capillary loops would seem likely candidates for SCCT. Their obliteration could account for the glomerular lobulation and simplification typically seen in advanced diabetic glomerulopathy. The frequency of SCCT in 1µm plastic sections and their absence in 4µm paraffin sections in the same case suggest that SCCT may be underrecognized.

1496 Mesangial Damage and Repair: The Role of Stem Cells. A 6D Living Cell Model.

J Teng, EA Turbat-Herrera, GA Herrera. Nephrocor, Tempe, AZ.

Background: In light chain deposition disease and AL-amyloidosis, mesangial cells are injured by GLCs resulting in MC apoptosis. However, the changes that occur in the mesangium are diametrically different. In AL-amyloidosis, mesangiolysis occurs whie in light chain deposition disease, the matrix increased and changes its compostion. Repair mechanisms of the affected mesangium are poorly understood. Stem cells may play an important role in repairing the damaged mesangium, especially since not many mesangial cells typically remain after the damage.

Design: Rat MCs were cultured on Matrigel loaded glass bottomed multi-well plates with 10% FBS/RPMI 1640 until confluence. MCs were then made quiescent by incubating them with 0.5% FBS/RPMI for 48 hours and then treated with LCDD and AL-AmLCs (10 ug/ml) purified from the urine of patients with renal biopsy proven conditions. Rat mesenchyma stem cells (RMSCs) are then stained with PKH-2 fluorescence or with Lysotracker Texas Red and placed 96 hours later into the wells of GLCs treated MCs for 2 weeks. The entire process is carefully monitored with sequential photos every 15 minutes using a 6D living cell model. This allows to observe the process of mesangial damage and how stem cells repair the damage.

Results: MCs treated with LCDD-LCs produced large amounts of matrix and formed nodules and those treated with AL-Am LCs engaged in the production of amyloid. MSCs cleaned up apoptotic MCs and eventually replaced injured cells becoming the majority of the cell mass. The amount of matrix material and amyloid decreased proportionally to the number of MSCs replacing the original MCs.

Conclusions: The reported observations with the 6D living cell imaging system demonstrated that the GLC-induced alterations are not irreversible and highlight a crucial role for MSCs replacing injured MCs and re-establishing mesangial homeostasis. In light chain deposition disease the process is complicated by the need to initially completely break down the abnormal accumulated matrix. These results suggest a therapeutic role for MSCs in repairing glomerular damage.

1497 Monitoring Graft Rejection Using Dual-Color Fluorescence Imaging of Formalin-Fixed Biopsies.

JE Tomaszewski, T Baradeti, JR Mansfield, M Feldman. University of Pennsylvania Health System, Pennsylvania; Cambridge Research & Instrumentation, Inc., Woburn, MA.

Background: Rejection is the major cause of graft failure, and if the injury to the organ is severe, it may not recover; prompt diagnosis of acute rejection is therefore important, with the monitoring of capillary C4d deposition being a good indicator. For renal biopsies in particular, obtaining this diagnosis has often required taking two biopsies, one for frozen-section analysis, the other fixed in formalin. Currently, immunofluorescence (IF) on frozen sections is the standard for immunochemical evaluation of renal biopsy specimens. IF labeling is not often used for formalin-fixed, paraffin-embedded (FFPE) specimens because of their inherent autofluorescence makes high-quality IF imaging difficult. Advances in spectral imaging algorithms can provide a simple means of overcoming autofluorescence interference, enabling the use of FFPE sections for renal image assessment and eliminating the need for dual biopsies. Vessels from biopsies from transplants can be marked using one label (e.g. CD34) and C4d another, and automated morphology-based image analysis used to obtain an objective assessment of rejection.

Design: A series of matched formalin-fixed and frozen renal biopsy specimens were sectioned and stained for CD34 and C4d, and IF images of them acquired using a spectral imaging system. Multispectral images were then unmixed and analyzed using an automated morphologic image analysis software package to assess C4d staining levels in capillaries. An image-based objective measure of rejection status was then developed and compared to visual assessment.

Results: High-quality IF images from FFPE specimens were obtained using spectral imaging to remove autofluorescence, and automated morphologic analysis of the images was able to identify vessels and quantify the C4d intensities within those regions. Results from formalin-fixed specimens were comparable to those from frozen, and the image-based objective measure of rejection status gave good correlation to visual assessment.

Conclusions: Automated assessment of dual-labeled (CD34 and C4d) FFPE renal biopsy specimens can be achieved using spectral imaging and morphologic image analysis software, and gives a good correlation with results from frozen sections and against visual assessment. This methodology shows promise for becoming a routine method for clinical assessment of organ transplant biopsies and is amenable to studies of archival tissue.

1498 Evaluation of Endothelial Cell Enlargement in Glomerulitis.

M Valente, L Furian, P Rigotti, M Della Barbera, F Marchini, S Marino, M Cardillo, FB Aiello. University of Padua, Medical School, Padova, Italy; Azienda Ospedaliera Padova, Padova, Italy; Azienda Ospedaliera ULSS 12, Venezia, Iraq; Centre for Organ and Tissue Transplant, IRCCS, Ospedale Maggiore, Milano, Italy; University of Chieti, Italy.

Background: Glomerulitis is defined by mononuclear cells in glomeruli and endothelial cell enlargement. In T cell mediated acute rejection, according to the Banff classification, glomerulitis is scored but not utilized to grade T cell mediated acute rejection, in contrast, in antibody mediated acute rejection its prognostic significance has been proposed to be relevant.

Design: Glomerulitis was studied in 90 consecutive acute rejections, time interval 2004-2009, matched as closely as possible for type and grade. CD68 and C4d immunostaining was performed in all cases. Glomerular endothelial cell enlargement (ECE) was measured morphometrically following CD31 immunostaining (ECE = endothelial cell area/total capillary area x 100)

Results: Glomerulitis was present in 36 cases (group 1) and absent in 54 (group 2). ECE was measured in 15 biopsies of group 1, 8 of group 2 and in 8 control biopsies with no evidence of rejection. The ECE mean value of group 1 (69.3 $\pm$ 6.7%) but not that of group 2 (58.5 $\pm$ 6.6%) was higher than in controls (57.0 $\pm$ 3.56%) ($P< 0.05$). C4d deposition, observed in 14/36 rejections of group 1 (38.9%) and in 7/54 rejections of group 2 (13.0%) ($P< 0.05$), was associated with steroid resistance (OR = 4.97 95% CI 1.76-14.02, $P< 0.05$). In patients with C4d+ rejections the presence of glomerulitis markedly increased the association (OR = 9.17, 95% CI 1.15-73.24, $P< 0.05$).

Conclusions: Our results indicate a significant endothelial cell enlargement in glomerulitis. In C4d+ acute rejection glomerulitis, associated with steroid resistance, may have an important prognostic significance.

1499 Hematologic Malignancies in Native Renal Biopsies: Report of 35 Cases.

CA VanBeek, CC Nast, AH Cohen, J Hussong, M Haas. Cedars-Sinai Medical Center, Los Angeles, CA.

Background: Primary renal hematologic malignancies are rare, while secondary renal involvement is a known complication of lymphomas and leukemias. As they seldom cause renal failure, leukemic/lymphomatous infiltrates of the kidney are rarely biopsied and their frequency in native kidney biopsies is not well documented.

Design: Of 13,828 non-transplant medical renal biopsies examined from 2004-2010, 35 with hematologic malignancies were identified. Light, immunofluorescence, and electron microscopies, immunohistochemistry, and clinical information were reviewed.

Results: There were 29 males and 5 females, ages 18 – 89 (mean 62). In 12 cases (34%) the renal biopsy provided the first diagnosis of malignancy including intravascular large B-cell (2), T-cell (2), diffuse large B cell (DLBCL) (4), chronic lymphocytic leukemia (CLL) and other low grade B-cell (4) lymphomas. Cases with prior neoplastic history included CLL and other low grade B-cell lymphomas (18), myeloid leukemia (2), DLBCL (1), and B-(1) and T-(1) acute lymphoblastic leukemia. The intravascular lymphomas involved glomerular capillaries causing hematuria and proteinuria, whereas the other 9 high grade lymphomas produced acute renal failure (ARF) with interstitial infiltration, often involving >80% of the parenchyma. One case of DLBCL also presented with nephrotic syndrome (membranous glomerulopathy). In contrast, low grade neoplasms typically involved <30% of the parenchyma and in 20/24 (83%) co-existing pathology was the cause of renal symptoms. In one case of CLL, atypical lymphocytes in glomeruli produced a membranoproliferative pattern without immune complexes, with hematuria and proteinuria. Ten cases of low-grade B cell lymphoma showed paraprotein-associated lesions, including 4 cases of immunotactoid glomerulonephritis (GN). Other concurrent lesions were minimal change nephropathy, immune complex GN, diabetic nephropathy, nodular glomerulosclerosis, pauci-immune crescentic GN and tubulo-interstitial diseases. Of the 2 myeloid leukemias, one showed neoplastic cells in 90% of the parenchyma with ARF, and in the other immature myeloid cells intermixed with inflammation of interstitial nephritis.

Conclusions: Hematologic malignancies were found in 0.25% of native renal biopsies performed to evaluate non-neoplastic diseases. In 1/3 of cases, the renal biopsy provided the first diagnosis of lymphoid neoplasm. High grade malignancies cause a variety of renal symptoms depending on histologic distribution. Low grade malignancies are typically incidental findings. Recognition of these neoplasms is important for appropriate clinical management.

1500 Spectrum of Renal Injury with Antiretroviral Therapy.

CA VanBeek, AH Cohen, M Haas, CC Nast. Cedars-Sinai Medical Center, Los Angeles, CA.

Background: Antiretroviral therapy (ART) agents are associated with various forms of renal injury. Nucleotide reverse transcriptase inhibitors (NtRTI) tenofovir (T), adefovir (Ad) and cidofovir (Cd) cause tubular mitochondrial injury; T is used in HIV while Ad and Cd are given for other viral infections. Nucleoside reverse transcriptase inhibitors (NsRTI) also may induce mitochondrial injury, while protease inhibitor indinavir (IDV) causes crystal deposition and rarely interstitial nephritis. We sought to assess the range of renal injury in biopsies from patients on ART.

Design: From 2000-2010, 101 biopsies from 101 patients on ART had adequate material and were included. Biopsies were evaluated by light (LM), immunofluorescence and electron (EM) microscopies, and available clinical and laboratory data were reviewed. Abnormal (A) tubular cell mitochondria (TCM) were defined as >1000 nm in width, with broken, absent or distorted cristae, and irregular non-uniform shape.

Results: Of 101 biopsies, 54 had ATCM. This included 38 of 57 (67%) patients on T with tubular cell damage (TCD) by LM and serum creatinine (Cr) from 1.5 to 14 (mean 4.7) mg/dl. Of those with available data, 53% had glycosuria with normal serum glucose. In patients taking ART other than T, 16 of 44 (29%) demonstrated ATCM and TCD with Cr from 1.5 to 8.5 (mean 3.5)mg/dl. One of these patients discontinued T 4 months prior to biopsy for nephrotoxicity, but had persistent renal failure. Other medications in this group included Cd for CMV retinitis (1), Ad for hepatitis B (2), NsRTIs for HIV (9) and 3 were on regimens without Ns- or NtRTIs. Ultrastructurally, affected tubular cells contained from a single to > 50% ATCM. Each involved tubule had from one to many (up to 70%) affected cells. By LM, tubules with TCD were clustered, and comprised from < 5% to > 50% of tubules. Other ART associated lesions included 2 cases of IDV-induced crystal-containing casts. The remaining 45 cases (18 on T, 27 not on T) had normal TCM and diagoses of ATN (24), ATN with interstitial nephritis (10), interstitial nephritis (9) and 2 without tubulo-interstitial injury.

Conclusions: ATCM are found in 54% of biopsies from patients receiving ART; of these, 30% occur in the absence of T treatment. Patients receiving Cd and Ad for non-HIV viral infections and those on ART other than NtRTI may develop this form of tubular damage. ATCM may occur in small numbers in few tubular cells, and patients with progressive renal failure may have only few affected cells. Therefore, careful ultrastructural evaluation is required in all patients receiving ART for identification of this lesion.

1501 Utility of Fluorescence *In Situ* Hybridization in Diagnosing BK Viral Nephropathy in Renal Allograft Biopsies.

Z Wang, BP Portier, JC Myles, A Chiesa-Vottero, R Neelon, G Procop, RR Tubbs. Cleveland Clinic, OH.

Background: BK nephropathy may complicate post transplant immunosuppression with potential graft loss if not appropriately managed. Early detection is essential to management which may include a reduction in immunosuppression. Conversely, if the cause of increasing renal insufficiency is acute rejection, immunosuppression may be increased. PCR based screening is sensitive and specific for BK virus detection within urine and blood, however fluorescence in situ hybridization (FISH) as a methodology to detect BK virus in formalin fixed paraffin embedded (FFPE) renal allograft tissue biopsies has not been previously evaluated.

Design: Data was retrieved from the Cleveland Clinic (CC) electronic medical record from 1/2005 to 12/2009 wherein patient's were included if they had a history of renal transplantation, subsequent renal biopsy preformed at CC, and documented blood or urine BK virus PCR performed concurrently at time of biopsy. A total of 40 patients were identified that met inclusion criteria. The presence or absence of viral inclusions on H&E as reviewed by medical renal pathologists (JLM and ACV) were recorded. FISH was then performed in both patient and positive control tissues using 1) a BK specific DNA probe (red) and 2) CEP8 centromeric probe (green) as a control for successful hybridization. Probe hybridization time was two hours, enabling same day resulting. FISH results were reported as positive or negative.

Results: FISH detected BK virus in 15 (38%) cases; while H&E viral inclusions within tubular epithelial nuclei were defined as positive in 3 cases (7.5%), suspicious in 15, and negative in 22. PCR performed on urine and blood identified BK virus in the same 15 cases that were identified by FISH, plus one additional case. The agreement between FISH and PCR was 97.5%. The agreement between the presence of viral inclusions on H&E and PCR was 67.5%. In relation to PCR, the sensitivity and specificity of FISH was 93.8% and 100% respectively. In relation to PCR, the sensitivity and specificity of finding viral inclusions on H&E was 18.8% and 100% respectively.

Conclusions: FISH performed for BK virus using FFPE renal allograft biopsies performs similarly to that of PCR based viral detection within blood and urine. The sensitivity of the FISH assay is superior to detection of BK viral inclusions on H&E stained slides. Finally, utilizing FISH for BK virus identification is straightforward, offers a short turn around time, and requires no variation from standard FISH protocol, thus making it a viable option for BK virus identification.

1502 Immunohistochemical (IHC) Staining with Kappa and Lambda Confirms Monoclonality Detected by Immunofluorescence Studies (IF) and Reveals a High Percentage of "Hybrid" Proximal Tubulopathy in Light Chain Associated Monoclonal Nephropathy (LCAMN).

W Wiesend, M Rooney, T Fennell, S Hicks, P Zhang. William Beaumont Hospital, Royal Oak, MI.

Background: Basic research studies have shown that monoclonal light chains, uptaken by megalin-cubilin receptors in proximal tubules, stimulate cellular production of hydrogen peroxide and induce an inflammatory process causing tubular injury. Monoclonal proximal tubulopathy, however, is a relatively rare variant of LCAMN, based on current EM diagnostic criteria in human renal biopsies. The purpose of this study was to 1) confirm IF findings by IHC method and 2) determine whether IHC method could reveal monoclonal light chain staining in proximal tubules of LCAMN cases.

Design: The study included 18 control cases (8 FSGS and 10 immune complex mediated glomerulopathy) and 23 LCAMN cases (9 cast nephropathy, 7 light chain deposition disease, 6 AL amyloidosis and 1 "pure" proximal tubulopathy). Staining pattern for kappa and lambda by IHC method was evaluated as polyclonal (equivalent kappa and lambda stains) and monoclonal (dominant kappa or lambda staining). The monoclonal staining in proximal tubules was also recorded. PAS staining of proximal tubular brush borders was graded from 0 (intact) to 3+ (total loss of brush border) in each case.

Results: All cases in the control group showed equivalent kappa and lambda stains indicating polyclonal pattern. All cases in the LCAMN group showed either kappa or lambda dominant staining, indicating monoclonal pattern, which was 100% correspondent with the monoclonal record by IF method. Monoclonal proximal tubular staining was seen in 8/9 cases of cast nephropathy, 7/7 cases of light chain deposition disease and one "pure" proximal tubulopathy, but in only 1/6 AL amyloidosis cases. The PAS scores of all LCAMN cases ranged from 2+ to 3+, except for the 5 AL amyloidosis cases without monoclonal staining in proximal tubules, which showed 0 to 1+ PAS scores. The mean value of serum creatinine in the LCAMN group was 4.89 ± 0.73 mg/dl, which significantly correlated with the PAS scores (R value: 0.496 and $p = 0.0136$).

Conclusions: IHC studies confirmed the monoclonal data identified on previous IF studies. In addition, IHC revealed a high percentage of "hybrid" monoclonal proximal tubulopathy (16/22 cases, 73%, not counting the "pure" proximal tubulopathy case), defined by monoclonal staining in proximal tubules and moderate to severe loss of brush borders. We conclude that monoclonal proximal tubulopathy, "pure" or "hybrid" type, may significantly contribute to acute renal failure in patients with LCAMN.

1503 Angiotensin II Type I Receptor Blocker Is Limited in Protection Against Severe Podocyte Injury-Induced FSGS.

H-C Yang, S-W Wang, I Pastan, T Matsusaka, I Ichikawa, AB Fogo. Vanderbilt University Medical Center, Nashville, TN; National Cancer Instiute, National Instiute of Health, Bethesda, MD; Tokai University Medical School, Isehara, Kanagawa, Japan.

Background: In 5/6 Nx models in both rats and mice, we found high dose angiotensin II type I receptor blocker (ARB) prevented glomerulosclerosis progression and even could induce regression. Nep25 mice, which express the human CD25 receptor on podocytes, can dose-dependently develop progressive glomerulosclerosis when immunotoxin (LMB2) is administered and binds this receptor. Previously we have shown that renal collagen I expression was parallel to luciferin imaging in double transgenic Nep25/collagen I-luciferase mice with glomerulosclerosis induced by this toxin. In this study, we aimed to examine if ARB could protect in this model of severe primary podocyte injury-associated FSGS.

Design: Collagen I-luciferase/Nep 25 mice were exposed to a mean dose of LMB2 toxin (12.5 ng/g BW, i.p.). Mice were biopsied at week 2, randomly assigned to the ARB

losartan (200mg/L) or not treated (control group), then sacrificed at week 6. Podocyte number, urine total protein/creatinine ratio, glomerulosclerosis index (SI, 0-4 scale) and collagen I associated luciferase activity were measured.
Results: LMB2 reduced podocyte number about 40% assessed by WT-1 staining (normal 7.50±0.50 *vs.* LMB2 4.64±0.11 /glomerulus). The control group showed edema and persistent proteinuria (week 2 66.06±14.51, week 4 72.52±11.40, week 6 87.33±29.57). Progressive glomerulosclerosis (SI, week 2 1.26±0.11 *vs.* week 6 1.81±0.04, $p<0.05$) and increased collagen I activity also developed (luciferase imaging score, week 2 0.84±0.13, week 4 1.66±0.09, week 6 1.79±0.001 $\times e^6$, $p<0.05$ overtime) in control toxin-treated mice. Losartan stabilized collagen I activity (luciferase imaging score, week 2 0.96±0.18, week 4 0.78±0.10, week 6 1.06±0.13 $\times e^6$). However, ARB did not decrease proteinuria (week 2 96.18±16.53, week 4 94.10±11.96, week 6 73.76±7.92, pNS) and did not prevent glomerulosclerosis progression (SI, week 2 1.48±0.15 *vs.* week 6 2.09±0.19, $p<0.05$).
Conclusions: Our data indicate that severe podocyte loss causes progressive glomerulosclerosis, and ARB alone cannot prevent glomerulosclerosis progression in this setting. This may be related to continuing podocyte loss cycle which accelerates the progression process.

1504 Green Tea Polyphenol (-)-Epigallocatechin-3-Gallate (EGCG) Ameliorates Experimental Immune-Mediated Glomerulonephritis.

T Ye, A Peng, D Rakheja, C Mohan, XJ Zhou. UT Southwestern Medical Center, Dallas, TX.
Background: Oxidative stress and inflammation play critical roles in the pathogenesis of immune-mediated glomerulonephritis (GN). The green tea catechins, particularly (-)-epigallocatechin-3-gallate (EGCG), are potent anti-inflammatory and anti-oxidant agents shown to inhibit leukocyte chemotaxis, quench free radicals, chelate transition metals, and interrupt lipid peroxidation chain reaction. It is estimated that EGCG is 25 times more potent than vitamin E and 100 times more potent than vitamin C making it an attractive compound for the treatment of diseases such as anti-GBM-GN that are characterized by severe immunologic and oxidative injury. However, the effect of EGCG on the clinical and pathological progression of immune-mediated renal injury has not been investigated.
Design: We tested the hypothesis that the anti-inflammatory and anti-oxidant properties of EGCG may favorably affect the course of immune-mediated GN using a murine model of anti-GBM-GN. 129/svJ mice were challenged with rabbit anti-mouse-GBM sera to induce GN and subsequently divided into EGCG (50 mg/kg/day, orally) and vehicle treated groups. Routine histology, markers of oxidative stress and key molecules associated with redox and inflammatory pathways were studied.
Results: Vehicle-treated mice developed glomerular crescents, tubulointerstitial disease and inflammatory cell infiltrates. EGCG treatment led to reduced proteinuria and serum creatinine and marked improvement in renal histology. Vehicle-treated mice showed increased oxidative stress [malondialdehyde (MDA), H_2O_2 and nitrotyrosine], elevated osteopontin (OPN), p65-NFκB, inducible nitric oxide synthase (iNOS), NO metabolites, superoxide dismutase (SOD), myeloperoxidase (MPO), p-Akt, and p47phox, and reduced PPARγ, glutathione peroxidase (GPx), and catalase activity. Treatment with EGCG led to a reduction in oxidative stress, normalization of OPN, p65-NFκB, iNOS, NO metabolites, p-Akt, p47phox, MPO, GPx, and PPARγ, and a significant increase in SOD expression.
Conclusions: our data suggest that EGCG ameliorates laboratory and histologic abnormalities in the mouse model of immune-mediated GN. These salutary effects of EGCG are likely mediated by the anti-inflammatory and anti-oxidative properties of this compound. These observations demonstrate the potential utility of EGCG as a novel therapeutic agent for the treatment of immune-mediated glomerulonephritides and various other immune-mediated diseases.

1505 Henoch-Schölein purpura Nephritis (HSPN) and IgA Nephropathy (IgAN) in Children: A Comparison of Pathological Features Using Oxford Classification of IgA Nephropathy.

X Zeng. Wayne State University, Detroit, MI.
Background: HSPN and IgAN are common in the pediatric population with overlapping clinical, genetic and immunological features causing HSPN to be considered as a systemic form of IgAN. Both entities are characterized by immunofluorescent IgA staining with variable degrees of mesangial proliferation and by IgA deposits on electron microscopy (EM). HSPN has been reported to show more severe glomerular lesions than IgAN however, systemic approach to quantitatively compare both diseases is lacking. The objective of this study was to assess the benefit of applying the newly described semi-quantitative, Oxford classification of IgA nephropathy (OXC-IGA), to distinguishing these two entities.
Design: All consecutive renal biopsy performed at the Children's Hospital of Michigan between 2004-2010 with a diagnosis of IgAN and HSPN were reviewed. The scoring system of OXC-IGA was applied to all biopsies to measure mesangial cellularity (MC, M score), segmental glomerulosclerosis (SG, S score), endocapillary hypercellularity (EC, E score) and tubular atrophy and interstitial fibrosis (TA/IF, T score). In addition, the highest number of MC, percentage of glomeruli with EC, cellular crescent (CC) and segmental necrosis (SN) were also recorded and compared between HSPN and IgAN using student t-test and basing statistical significance of $P<0.05$.
Results: A total of 23 HSPN (F:M=12:11) and 26 IgAN (F:M=11:15) were diagnosis during the study period. The HSPN patients were significantly younger than IgAN (7.8+/-3.3 vs 12.4+/-3.2, years, $p<0.05$). Patients with HSPN had significantly higher MC (11 3.2 vs 8.3 2.4), percentage of EC (14.9 2.2 vs 4.9 8.2), CC (10.4 1.2 vs 4.3 2.8) and SN (6.6 1.3 vs 0.7 1.1, all with a $P<0.05$). There was no significant difference between IgAN and HSPN in M, S, E and T score ($p>0.05$).

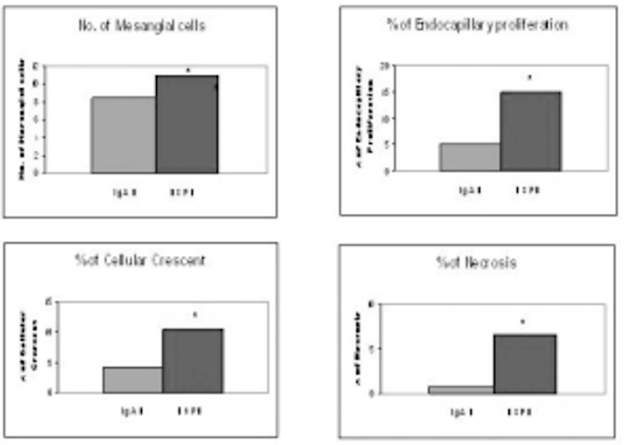

Conclusions: While our data showing IgAN and HSPN to share histopathological features of mesangial/endocapillary proliferation, we demonstrated that HSPN has more extensive mesangial/endcapillary proliferation, high percentage of glomeruli with cellular crescent and segmental necrosis, thus more severe glomerular damage. These findings further characterize pediatric HSPN, therefore benefit to the clinical management.

1506 Histopathologic Characteristic of Pediatric Anti-Neutrophil Cytoplasmic Antibody-Associated Glomerulonephritis (ANCA-GN).

X Zeng. Wayne State University, Detroit, MI.
Background: ANCA-GN is the most common cause of rapidly progressive glomerulonephritis (GN) and the diagnosis is made by renal biopsy. Most ANCA-GN patients are adults. The recently published "histopathologic classification of ANCA-GN" by Annelies et al (J Am Soc Nephrol 21, 2010 e-publish) divides ANCA-GN into four categories (focal, crescentic, mixed and sclerotic ANCA-GN) corresponding to the severity of renal function impairment and outcome. Based on this classification, the majority of adult ANCA-GN belongs to the crescentic group, which has highly active renal disease and severely reduced renal function. There is paucity of reports regarding pediatric ANCA-GN, especialy those corrlating histopathologic changes and outcome. The objective of this study is to charaterize histopathologic changes and outcome in pediatric ANCA-GN.
Design: Renal biopsy cases with a diagnosis of ANCA-GN from pathologic database of Children's Hospital of Michigan between 2004-2009 were reviewed. Based on the predominance of normal glomeruli, cellular crescents and globally sclerotic glomeruli, ANCA-GN case was classified into one of the four categories listed above. In addition, the activity index and chronicity index for each ANCA-GN, including percentage of cellular crescent, segmental necrosis, global sclerotic glomeruli and tubular atrophy and interstitial fibrosis (TA/IF) were recorded.
Results: During the study time frame we identified 7 ANCA-GNs (F:M=4:3). The children ranges from 8-17 year-old (mean age 13.4). Five of 7 cases were focal ANCA-GN (71%) and two were crescentic (29%). None was mixed or sclerotic. Four of 7 ANCA-GN patients carried the diagnosis of Wegener's granulomatosis. The average percentage of crescent, necrosis, global sclerotic and TA/IF was 3.5%, 1.7%, 1.3% and 20, respectively.

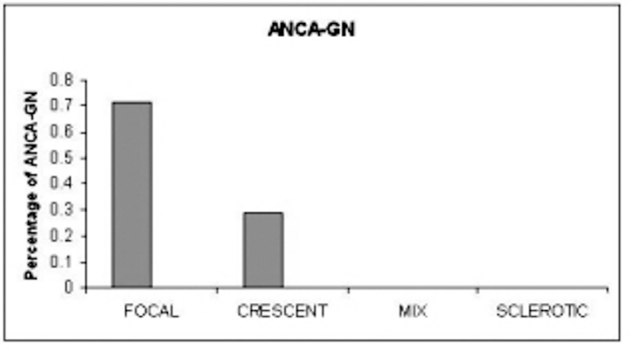

Conclusions: The majority of pediatric ANCA-GN have focal disease, and therefore has a favorable renal outcome compared to adult ANCA-GN. The pediatric ANCA-GN has mild activity index including small percentage of cellular crescents and segmental necrosis. The chronicity index is also low in pediatric ANCA-GN with lower number of global sclerotic glomeruli and lower TA/IF.

1507 The Expression of Apoptotic Related Proteins and Apoptosis in Human Renal Tissues of Class II and IV Lupus Nephritis.

J Zhang, J Cui, YQ Zhang, Q Qiao. Xijing Hospital, Fourth Military Medical University, Xi'an, Shaanxi, China; Tangdu Hospital, Fourth Military Medical University, Xi'an, Shaanxi, China.

Background: Apoptosis is involved in glomerular injuries leading to glomerulonephritis. The role of renal cell apoptosis in the pathogenesis and progress of human lupus nephritis (LN) is still controversial. Furthermore, in different types of LN renal tissues, the expression of apoptotic related proteins, such as FasL, Bax and caspase-3, is still unknown. We therefore investigated these apoptotic related proteins and apoptosis index (AI) in human renal tissues of class II and IV LN.

Design: The expressions of FasL, Bax and caspase-3 were assessed in forty-two cases of human LN renal tissues (twenty cases of class II, twenty-two cases of class IV) and ten cases of human normal renal tissues by immunocytochemistry. The terminal deoxynucleotidyl transferase dUTP nick end labeling (TUNEL) staining was used to assess AI.

Results: In class II and IV LN renal tissues, the increased expressions of FasL, Bax, caspase-3, and AI were detected in glomerular cells, tubular epithelial cells compared with controls (P<0.05). The expression of Bax, caspase-3 and AI in glomerular cells of class IV LN was significantly higher than class II LN (P<0.05). However, there was no difference in FasL expression between class II LN and class IV LN (P>0.05).

Conclusions: Apoptosis might be induced to LN pathogenesis by FasL, Bax and caspase-3. There might be other pathways except Fas/FasL signaling to initiate apoptosis during LN progress.

1508 Exogenous Ac-SDKP Administration Regulates Profibrotic Molecules in Obstructed Kidneys.

Y Zuo, SA Potthoff, H-C Yang, L-J Ma, AB Fogo. Vanderbilt University, Nashville, TN.

Background: Our previous studies showed that thymosin β4 (Tβ4), a G-actin sequestering protein, is remarkably increased in the obstructed kidney in the unilateral ureteral obstruction (UUO) model of tubulointerstitial fibrosis. Ac-SDKP, the degradation product of Tβ4 by prolyl oligopeptidase (POP), is postulated to have anti-fibrotic effects. Moreover, we found that inhibition of POP shifted the balance of Tβ4 and Ac-SDKP and exacerbated fibrosis in obstructed kidneys. We have now investigated profibrotic molecular gene expression in the UUO kidneys.

Design: Male C57BL/6 mice were sacrificed at day 5 after UUO and treatments: UUO without treatment, UUO+POP inhibitor (S17092, 40mg/kg per day, by gavage), UUO+Tβ4 (150μg/d, i.p.), UUO+combination (POP inhibitor and Tβ4), and UUO+Ac-SDKP (1.6 mg/kg/d, delivered by minipump).

Results: POP activity was significantly decreased in the obstructed kidneys of mice treated with either POP inhibitor or the combination (8% and 21% of levels in untreated UUO, respectively, both p<0.05). Ac-SDKP concentration was significantly reduced by both the POP inhibitor and combination treatment but dramatically increased by Ac-SDKP administration vs. untreated UUO (POP inhibitor, 47%; combination, 61%; Ac-SDKP, 172% of untreated UUO, respectively, all p<0.05). Neither POP activity nor Ac-SDKP was affected by Tβ4 treatment (77% and 78% of untreated UUO, respectively). Ac-SDKP treatment dramatically decreased plasminogen activator inhibitor (PAI-1), transforming growth factor (TGF)-β1, Tβ4, collagen I and III expression assessed by real time PCR vs. untreated UUO. By contrast, PAI-1, TGF-β1 and collagen III expressions were significantly increased by POP inhibitor. Ku80, a potential receptor for Tβ4, was abundantly present in glomerular endothelial cells and peritubular capillary endothelium in UUO kidneys and increased vs. non-obstructed kidneys. Ku80 mRNA in the UUO kidney assessed by real time PCR was dramatically increased by POP inhibitor and Tβ4 treatment vs. untreated UUO.

Conclusions: Our study suggests that exogenous administration of Ac-SDKP inhibits profibrotic factors. We propose that the balance of thymosin β4 and Ac-SDKP is crucial in determining tubulointerstitial fibrosis, and Ku80, a potential receptor for Tβ4, may modulate these processes.

Liver & Pancreas

1509 Site-Specific Subclassification of Ampullary Carcinomas: Delineation of Four Clinicopathologically and Prognostically Distinct Subsets in an Analysis of 249 Cases.

N Adsay, N Ohike, T Tajiri, GE Kim, A Krasinskas, S Balci, O Basturk, S Bandyopadhyay, DA Kooby, SK Maithel, J Sarmiento, CA Staley. Emory, GA; Showa, Yokohama, Japan; UCSF, San Francisco, CA; UPMC, Pittsburgh, PA; MSKCC, NY; WSU, MI.

Background: Ampullary (AMP) carcinomas (ACs) encompass a highly heterogeneous group; there have not been uniformly applied definitions or systematic analysis of the neoplasms arising in different compartments of this region.

Design: 249 strictly-defined primary ACs were analyzed with careful correlation of gross and microscopic findings to determine the tumor epicenter, and if present, extent of involvement by preinvasive neoplasm of the duodenal surface (DS), the edge of papilla of Vater (PV) and intraampullary region (IA). Their prognosis was compared to that of 112 pancreatic carcinomas.

Results: I. Overall, AC cases had significantly better prognosis than pancreatic carcinoma cases (p<0.01). **II.** ACs could be further classified into 4 distinct subtypes (See figure 1 for illustration and clinicopathologic information). **1.AMP-NOS**: Ulcero-fungating tumor located at PV with epicenter of invasion at PV/IA was most common (56%). **2.Intra-AMP:** Invasive carcinomas arising in intraampullary papillary-tubular neoplasms (AJSP, 2010, in press) had the best prognosis. These relatively large overall sized tumors had smaller size of invasion and typically occurred in men. **3.AMP-ductal**: Mucosal-covered, button-like elevation of PV without significant exophytic (preinvasive) growth on DS/PV had plaque-like thickening of intrapancreatic CBD or pancreatic duct walls that formed constructive sclerotic (non-exophytic) tumors. These were the smallest tumors, but had the worst prognosis, presumably due to pancreatobiliary histology/origin, yet prognosis was better than pancreatic carcinomas (p<0.01). **4.PeriAMP-duodenal:** Exophytic (ulcero-fungating) duodenal tumor encasing PV but with bulk of preinvasive tumor (>75%) involving DS, and invasion epicenter away from ampulla itself. These were fairly large tumors with intestinal phenotype and high incidence of LN metastases.

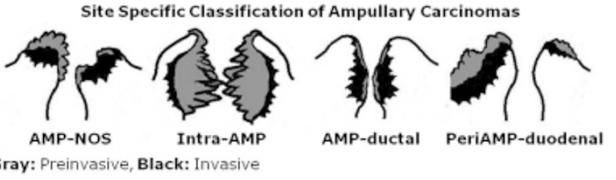

Clinicopathologic Data of Subtypes

	N	Age (y)	M/F	Mean size (mm) Overall/Inv	Invasive Histology (IN/non-IN)	LN Met (%)	T-stage T1+T2/ T3+T4	Survival (median mos/3y%)
AMP-NOS	140	65	1.5	25/18	38/102*	42	86/54	30*/45
Intra-AMP	61	64	2.2	29/15^	33/28^	28	52/9^	50^/69^
AMP-ductal	36	69*	0.9	19^/17	2/34^	41	14/22^	28/32
PeriAMP-duodenal	12	59	1.0	47^/34^	9/3^	50	8/4	46/63

p *<0.05 and ^<0.01; IN=Intestinal; LN=Lymph node; Met=Metastasis

Conclusions: AC comprises 4 clinicopathologic subtypes (*AMP-NOS, intra-AMP, AMP-ductal* and *PeriAMP-duodenal*) that are prognostically distinct.

1510 High Prevalence of IgG4 Positive Immunohistochemical Cholangitis in Liver Explants from Patients with PSC.

S Ali, GM Hirschfield, C Meaney, PD Greig, G Therapondos, SE Fischer. University of Toronto, ON, Canada.

Background: IgG4 associated cholangitis/pancreatitis is a highly steroid responsive inflammatory disease. As many as 10-15% of patients with primary sclerosing cholangitis (PSC) are reported to have elevated serum IgG4 levels, and this subpopulation may have a different natural history. IgG4 deposition histologically has been reported in explants from patients with PSC. The aim of the study is to confirm the prevalence of histological IgG4 associated cholangitis in patients undergoing liver transplantation for PSC.

Design: IgG4 immunohistochemistry was performed on liver explants from patients with PSC (n=123) and unrelated cholestatic and viral liver disease (n=50), using representative sections from the hilum. Positive IgG4 staining was defined either as ³10 positive IgG4 cells per high power field (HPF) or as no staining (<5 cells/HPF), mild staining (5-10 cells/HPF), moderate staining (11-29 cells/HPF) and marked staining (³30 cells/HPF). Immunochemical staining was compared to baseline lymphoplasmacytic inflammation. Clinical correlations with pre- and post-transplant variables were performed.

Results: Of the 50 control liver sections (PBC, n=19; HCV, n=19; HBV, n=8; AIH, n=6) none had marked staining and mild-moderate staining was seen in only one AIH explant, one PBC explant, and three HCV explants. In contrast of the 123 explants from patients with PSC studied, 59 (48.0%) had positive IgG4 immunohistochemical staining in hilar tissue (³10 cells per HPF). Forty two (34.1%) were classified as no IgG4 staining, 22 (17.9%) had mild staining, 28 (22.8%) moderate staining, and 31 (25.2%) had marked staining. Tissue IgG4 positivity was strongly correlated with moderate to marked periductal (hilar) lymphoplasmacytic inflammation (P<0.001) i.e. the inflammation surrounding the large hilar ducts which extends into adjacent tissue. Positive IgG4 staining was more likely in men (P=0.04), and in those with a history of pancreatitis (P=0.03). Other clinical parameters were unrelated to IgG4 staining, in particular age at diagnosis, presence of IBD and presence of recurrent disease.

Conclusions: A large number of patients undergoing transplantation for PSC have marked histological IgG4 plasmacytic cholangitis. Further characterization of the significance of this histological observation is required, as it raises the question of whether steroids may have a role in a sub-population of patients with PSC.

1511 Antibody-Mediated Rejection and Graft Outcome in ABO-Compatible Liver Re-Transplantation.

S Ali, V Shah, K Kantz, A VanDyke, M Mahan, S Skorupski, B Eisenbery, I Lopez-Plaza, G Rada, A Ormsby. Henry Ford Hospital, Detroit, MI.

Background: Unlike kidney, the role of HLA antibody mediated rejection (AMR) in ABO-compatible liver transplantation is still controversial. Limited reports described isolated episodes of AMR with early graft loss requiring re-transplantation (re-tx) despite aggressive therapy. We conducted a retrospective study of re-transplanted patients (pts) to explore similar incidence and effect on transplantation outcome.

Design: Fifty four of 63 Pts who underwent ABO-compatible/identical orthotropic liver re-tx since May 2004 were selected. Pts were classified based on time to graft failure into group; (A) primary non-function graft or graft loss within the first 7 days (ds) from transplantation; (B) re-tx pts within 8-90 ds and (C) re-tx pts > 91 ds. The latter was chosen sequentially based on the UNOS registration number. 142 graft biopsies